Award Number: W81XWH-12-1-0062

TITLE: Molecular Determinants of Hormone-Refractory Prostate Cancer

PRINCIPAL INVESTIGATOR: Atish Choudhury

CONTRACTING ORGANIZATION: Dana-Farber Cancer Institute, Inc.
Boston, MA 02115-6013

REPORT DATE: July 2015

TYPE OF REPORT: Annual Summary

PREPARED FOR: U.S. Army Medical Research and Materiel Command
Fort Detrick, Maryland 21702-5012

REPORT DOCUMENTATION PAGE

Form Approved
OMB No. 0704-0188

1. REPORT DATE	2. REPORT TYPE	3. DATES COVERED
July 2015	Annual Summary	1 July 2014 – 30 June 2015

4. TITLE AND SUBTITLE
Molecular Determinants of Hormone Refractory Prostate Cancer

5a. CONTRACT NUMBER

5b. GRANT NUMBER
W81XWH-12-1-0062

5c. PROGRAM ELEMENT NUMBER

6. AUTHOR(S)
Atish Choudhury

E-Mail: achoudhury@partners.org

5d. PROJECT NUMBER

5e. TASK NUMBER

5f. WORK UNIT NUMBER

7. PERFORMING ORGANIZATION NAME(S) AND ADDRESS(ES)

Dana-Farber Cancer Institute
450 Brookline Ave
Boston, MA 02215

8. PERFORMING ORGANIZATION REPORT NUMBER

9. SPONSORING / MONITORING AGENCY NAME(S) AND ADDRESS(ES)
U.S. Army Medical Research and Materiel Command
Fort Detrick, Maryland 21702-5012

10. SPONSOR/MONITOR'S ACRONYM(S)

11. SPONSOR/MONITOR'S REPORT NUMBER(S)

12. DISTRIBUTION / AVAILABILITY STATEMENT
Approved for Public Release; Distribution Unlimited

13. SUPPLEMENTARY NOTES

14. ABSTRACT

We have performed a high throughput, *in vivo* genetic screen to identify kinases that permit androgen-dependent transformed prostate epithelial cells (LHSR-AR cells) to form tumors in female animals. In addition to known prostate cancer oncogenes and mediators of androgen independence (mutated KRAS, constitutively active MEK, RAF1, ERBB2, AKT1, PIM1 and PIM2), overexpression of the Never In Mitosis A (NIMA) related kinase 6 (NEK6) reproducibly yielded androgen-independent tumors. NEK6 is overexpressed in prostate cancer cell lines compared to their normal counterparts and is overexpressed in a subset of human prostate cancers. Expression of NEK6 confers castration resistance to established tumors in male mice, and suppressing NEK6 expression restores sensitivity to castration. Castration-resistant tumors generated through NEK6 overexpression are predominantly squamous in histology and do not express androgen receptor (AR), and NEK6 does not activate AR signaling. Phosphoproteome and interactome analysis reveals the transcription factors FOXJ2 and NCOA5, as well as the kinases CK1α and YES1 to be novel substrates. The gene expression profile mediated by NEK6 overexpression in tumors from castrated mice demonstrates elements of both differentiation and immune signaling, and phosphomimic forms of FOXJ2, YES1, and CK1α (but not NCOA5) recapitulate elements of this signature, particularly CK1α with markers of squamous differentiation. These studies reveal a novel mechanism of resistance in androgen pathway independent prostate cancer (APIPC).

15. SUBJECT TERMS
Prostate cancer, hormone refractory, castration resistant, androgen independent, NEK6

16. SECURITY CLASSIFICATION OF:			17. LIMITATION OF ABSTRACT	18. NUMBER OF PAGES	19a. NAME OF RESPONSIBLE PERSON
a. REPORT	b. ABSTRACT	c. THIS PAGE			USAMRMC
U	U	U	UU	47	19b. TELEPHONE NUMBER *(include area code)*

Table of Contents

INTRODUCTION

The interrogation of tissue obtained from patients with castration-resistant prostate cancer (CRPC) reveal molecular changes associated with this disease state; however, our understanding of signaling pathways functionally leading to castration resistance remains incomplete. Here we have performed a high throughput, *in vivo* genetic screen to identify kinases that permit androgen-dependent transformed prostate epithelial cells (LHSR-AR cells) to form tumors in female animals. In addition to known prostate cancer oncogenes and mediators of androgen independence (mutated KRAS, constitutively active MEK, RAF1, ERBB2, AKT1, PIM1 and PIM2), overexpression of the Never In Mitosis A (NIMA) related kinase 6 (NEK6) reproducibly yielded androgen-independent tumors. NEK6 is overexpressed in prostate cancer cell lines compared to their normal counterparts and is overexpressed in a subset of human prostate cancers. Expression of NEK6 confers castration resistance to established tumors in male mice, and suppressing NEK6 expression restores sensitivity to castration. Castration-resistant tumors generated through NEK6 overexpression are predominantly squamous in histology and do not express androgen receptor (AR), and NEK6 does not activate AR signaling. Phosphoproteome and interactome analysis reveals the transcription factors FOXJ2 and NCOA5, as well as the kinases CK1α and YES1 to be novel substrates. The gene expression profile mediated by NEK6 overexpression in tumors from castrated mice demonstrates elements of both differentiation and immune signaling, and NEK6 maintains the expression of a set of genes, including genes involved in interferon signaling, decreased with castration in this model. Phosphomimic forms of FOXJ2, YES1, and CK1α (but not NCOA5) recapitulate elements of the NEK6 gene expression signature, and the phosphomimic CK1α signature in particular correlates highly with the NEK6 signature with regards to expression of markers of squamous differentiation, such as KRT13. These studies reveal NEK6/CK1α signaling as one mechanism of resistance in androgen pathway independent prostate cancer (APIPC).

BODY

Background

Prostate cancer is the second most common cause of cancer death in men, and the majority of these deaths occur in patients with metastatic castration-resistant prostate cancer (CRPC). Clinical responses to agents that decrease circulating androgens to below castrate levels (abiraterone – Attard *et al.*, 2009) and new potent antagonists of the androgen receptor (enzalutamide – Scher *et al*., 2012) demonstrate that the androgen receptor (AR) signaling pathway remains critical in CRPC. Recent reports from studies of metastatic tissue in patients who have progressed on these therapies reveal that tumors can become resistant either through persistent activation of the AR pathway, or by progression to a state described as androgen pathway independent prostate cancer (APIPC) (Nelson, 2012), with or without evidence for neuroendocrine transdifferentiation.

Constitutive activation of kinases such as ERBB2, MAPK, PI3K/Akt, and Src (Edwards and Bartlett, 2005b) has been implicated in mediating resistance to hormonal therapies through both AR-dependent (Lin *et al*., 2001; Yeh *et al*., 1999; Guo *et al*., 2006), and AR-independent mechanisms (Pienta and Bradley, 2006). A number of recent studies have demonstrated the complementarity and crosstalk between kinase signaling pathways and AR signaling. Mendiratta, *et al*. (2009) developed a gene expression signature of AR signaling, and found that decreased predicted AR activity in patient samples correlated with increased predicted Src activity. Carver, *et al*. (2011) and Mulholland, *et al*. (2011) demonstrated cross-regulation through reciprocal feedback between the AR and PTEN/PI3K/MTOR signaling pathways. However, inhibitors of many of these kinases have failed to demonstrate significant clinical benefit in unselected patient populations, such as in trials of the ERBB2 inhibitor lapatinib (Whang *et al*., 2011), the MTOR inhibitor everolimus (Nakabayashi *et al*., 2012), and the SRC inhibitor dasatinib (Araujo *et al*., 2013). An agent targeting MET and VEGFR2, cabozantinib, has demonstrated interesting clinical activity in metastatic CRPC (Smith *et al*., 2014), but has not demonstrated improvements in overall survival or bone pain in randomized phase III trials.

Tumor samples from patients with CRPC have increased levels of tyrosine phosphorylation as compared to treatment naïve prostate cancer (Drake, *et al*. 2012; Drake *et al.,* 2013), and analysis of serine/threonine and tyrosine phosphorylation events in metastatic CRPC suggests particular signaling networks involved in this transition (Yazdi, *et al*. 2014). However, there is limited evidence for activating kinase point mutations in CRPC, suggesting that kinase pathways are activated by other (structural genetic, epigenetic, microenvironmental) mechanisms. Kinase signaling pathways whose activation could lead to castration resistance in patients have not been comprehensively catalogued, so we have performed an *in vivo* functional genomic screen to identify novel pathways that may be involved. These studies would help identify novel targets for therapeutic intervention (either the kinases themselves, or upstream/downstream mediators) and help with biomarker development for stratifying patients for likelihood of response to therapy.

We hypothesize that novel signaling pathways may be involved in conferring castrate resistance, and given that kinases usually act as transducers of growth and proliferation signals, we hypothesize more specifically that activated/amplified kinases play a role in the development of castration resistance. We have thus performed an *in vivo* functional genomic screen to identify novel pathways that may be involved and likely serve as therapeutic targets in these patients.

Previous work in our laboratory (Berger *et al*., 2004) demonstrated that primary prostate epithelial cells (PrECs) that are rendered tumorigenic by the expression of the SV40 large T and small t antigens, the catalytic subunit of telomerase (hTERT), H-Ras, and the androgen receptor (LHSR-AR cells) form well-differentiated tumors in mice. These tumors are androgen-dependent and are thus unable to grow in female or castrated mice. I have performed a high throughput, *in vivo* genetic screen to identify kinases that permitted these cells to form tumors in female animals. A lentivirally delivered kinase ORF library encompassing 601 kinases and other oncogenes was introduced into these cells in pools of 9-10, and I identified fourteen ORF integrants that allowed for the androgen-independent development of subcutaneous tumors by PCR using vector specific primers (Table 1). Using the same ORF library, I performed an *in vitro* screen for genes conferring androgen-independent proliferation to androgen dependent LNCaP cells and identified 13 genes that significantly (>2 standard deviations from median) increased proliferation in androgen-deprived conditions (Table 1).

The 24 total candidates identified from both screens were introduced into LHSR-AR cells individually and injected into 6 subcutaneous sites of female BALB/C nude mice for validation of androgen-independent tumor formation. Among the candidates that reproducibly yield androgen-independent tumors are mutated KRAS; RAF1, which is recurrently translocated (Palanisamy *et al*. 2010) and amplified (Taylor *et al*., 2010) in advanced prostate cancer; ERBB2, AKT1, and constitutively active MEK1, which have been implicated in androgen independence (Edwards and Bartlett, 2005a); and PIM1 and PIM2, which have previously been demonstrated to be important oncogenes in prostate cancer (Brault *et al*., 2010). Among the strongest candidates identified to confer androgen independence in this assay are the Never In Mitosis A (NIMA) related kinase 6 (NEK6), and nemo-like kinase (NLK).

Aim 1. Elucidating the role of NIMA-related kinase 6 (NEK6) and nemo-like kinase (NLK) as mediators of castrate-resistant prostate cancer and assessing their potential as therapeutic targets.

Milestone 1: Determine whether NEK6 and NLK can confer castrate resistance to established tumors, whether kinase activity is required, and whether their continued expression is required.

In addition to conferring tumor formation in female mice, overexpression of NEK6 in LHSR-AR cells also lead to tumor formation in castrated mice, which lack circulating androgens since mice do not synthesize androgens from their adrenal glands (Figure 1A). The tumors in castrated mice are generally smaller and slower growing than those in female mice, suggesting that signaling mediated by androgens play a role in the growth of the tumors even though they are not essential for tumor formation. In addition, we tested whether NEK6 overexpression can lead to androgen-independent tumor formation in a different genetic context, that is in immortalized PrECs transformed by overexpression of the MYC oncogene and expression of an active form of the p110α subunit of PI3 kinase (rather than with

Table 1. Results of *in vivo* and *in vitro* screens for genes conferring androgen independence, and of *in vivo* validation.

In vivo LHSR-AR screen		*In vitro* LNCaP screen		*In vivo* validation	
ORF	# tumors	ORF	Fold proliferation (× median)[b]	ORF	# tumors
KRASV12+MEKDD[a]	3/3	**NLK**	2.09	KRASV12	6/6
ERBB2	3/3	CDK6	1.90	ERBB2	5/6
NEK6	3/3	PIM1	1.72	**NEK6**	5/6
RAF1	3/3	CDK4	1.55	**NLK**	4/6
AKT1	1/3	PIM2	1.45	MEKDD	4/6
BRD3+NEK8[a]	1/3	STK40	1.44	AKT1	3/6
PIM2	1/3	RPS6KA2	1.40	RAF1	3/6
GK	1/3	AGK	1.40	PIM1	3/6
PFKP	1/3	TGFBR1	1.40	PIM2	1/6
PRKG2	1/3	DAPK3	1.39	others	0/6
TGFBR2	1/3	LOC389599	1.38		
PIM1	1/3	NEK5	1.37		
		AKT1	1.37		

[a] Two ORF integrants were amplified from these tumors

[b] For reference, the synthetic androgen R1881 leads to median 2.06 fold proliferation

small t antigen and active HRAS), termed LHMK-AR cells. Indeed, NEK6 overexpression led to tumor formation in this other genetic context (Figure 1B); however given that the tumors were smaller and somewhat less robust than those formed from LHSR-AR cells, functional studies performed below focused on tumors formed from the latter cells.

. As reported in previous Annual Summary Reports, the kinase activity of NEK6 is required for castration-resistant tumor formation, as a kinase dead version with mutations of lysine residues at amino acids 74 and 75 to methionine (K74M/K75M) did not confer this phenotype. To assess whether NEK6 could serve as a therapeutic target in established tumors where its activity is increased, we implanted cells with doxycycline-inducible expression of NEK6 (Figure 1C) in male mice with a testosterone pellet, and tumors were allowed to form in the presence of doxycycline in the diet. After 35 days, the mice were castrated, testosterone pellets was removed, and doxycycline was either continued or withdrawn (5 mice = 15 tumors per group; mice that died perioperatively were excluded from the analysis). We found that at day 30 after castration NEK6 confers resistance to castration compared to the parental cells when its expression is maintained with doxycycline ($p=0.001$) but sensitivity to castration is restored when doxycycline is withdrawn ($p=0.049$) (Figure 1C).

The tumors formed due to NEK6 overexpression have regions of nuclear AR expression but the majority of these tumors lacked AR expression (Figure 2A). Hematoxylin and eosin (H&E) staining demonstrates squamous differentiation in these tumors with the more mature differentiated regions demonstrating keratin deposition and AR loss. Androgen-independent tumors derived from expression of the other kinases identified in the screen also have regions of AR-positivity and negativity that vary in proportion and intensity (Supplemental Table 1). NEK6 overexpressing tumors established in male mice demonstrate strong nuclear AR staining with no squamous differentiation (Figure 2B, left panels). However, after castration, these tumors lose nuclear AR over time and develop more keratinization between nests of tumor cells (Figure 2B, bottom panels). This observation suggests that NEK6-mediated castration resistance does not require AR activity, and that transdifferentiation to a squamous phenotype is a result of or response to castration.

Milestone 1: NEK6 can confer castrate resistance to established tumors, kinase activity is required, and continued expression is required. The NEK6-mediated castration-resistant tumors are AR negative and squamous in histology.

Aim 2: Assessing signaling pathways involved in NEK6 and NLK-mediated castrate resistance and assessing their clinical relevance.

Milestone 2: Determine whether AR and STAT3 are necessary to confer NEK6 and NLK-mediated castrate resistance

Milestone 3: Determine impact of NEK6 and NLK on AR and STAT3 compared to other hits in the screen in vitro and in vivo

Given that persistence of AR signaling has been demonstrated to be an important mechanism of castration resistance, we sought to determine if NEK6 influences AR signaling. As noted previously, the NEK6-mediated castration resistant tumors lack expression of the AR, making it unlikely that AR is responsible for this phenotype. NEK6 overexpression does not lead to an increase in activity of an AR reporter based on the PSA enhancer in LNCaP cells (Supplemental Figure 2A), and inducible overexpression of NEK6 in LHSR-AR cells (Supplemental Figure 2B) does not lead to increased expression of the AR targets PSA and TMPRSS2 (Supplemental Figure 2C). Gene set enrichment analysis (Subramanian *et al*., 2005) of an mRNA expression signature of NEK6 activity generated from cells inducibly expressing wild-type vs. a kinase dead NEK6 form of NEK6 (with lysine resides at positions 74 and 75 mutated to methionine – O'Regan and Fry, 2009) *in vitro* demonstrates that gene expression changes associated with NEK6 kinase activity do not correlate positively or negatively (Supplemental Figure 2D) with three previously published signatures of AR activity (Hieronymus *et al*., 2006; Mendiratta *et al*., 2009; Sharma *et al.,* 2013).

It has previously been demonstrated that xenograft tumors with squamous histology can also be generated by transformation of patient-derived prostate basal cells (Stoyanova *et al*., 2013) with these tumors marked by active β-catenin; however there is no evidence for nuclear β-catenin staining in the NEK6-mediated castration resistant tumors generated here (Supplemental Figure 3A). Thus, we sought to determine whether other canonical oncogenic signaling pathways previously reported to be activated by NEK6 may be playing a role. NEK6 purified from rat liver was found to be the major protein kinase that is active on the p70 S6 kinase (RPS6KB1) hydrophobic regulatory site, Thr412 (Belham *et al*., 2001). Subsequently, it was demonstrated that NEK6 could phosphorylate hydrophobic motifs of RPS6KB1 as well as SGK1 *in vitro* (Lizcano *et al*., 2002). In addition, STAT3 phosphorylation at serine 727 has been implicated in the

transformation activity of NEK6 previously (Jeon *et al*., 2010). However, inducible expression of NEK6 in LHSR-AR cells does not increase phosphorylation on RPS6KB1 at Thr412 or STAT3 at Ser727 with or without growth factor stimulation as compared to cells expressing kinase-dead NEK6 or GFP (Supplemental Figure 3B). We were not able to find a quality antibody recognizing Ser422 of SGK1, but we were unable to demonstrate phosphorylation of SGK1 at Ser422 by active recombinant NEK6 in an *in vitro* kinase assay (data not shown).

Because NEK6 has previously been described to play a role in the G2/M transition (Yin *et al*., 2003) with its proliferative effects in hepatocellular carcinoma reported to be mediated through modulation of cyclin B (Zhang *et al*., 2014), we assessed whether NEK6 overexpression can influence cell cycle progression in our system. The baseline cell cycle profile is identical for cells with inducible expression of NEK6 with and without doxycycline in normally cycling cells, cells starved in growth-factor free media, and in cells released into growth-factor containing media (Supplemental Figure 4A). NEK6 does not increase proliferation rate of LHSR-AR cells *in vitro* compared to a lacZ control (Supplemental Figure 4B). Thus, the functional role of NEK6 overexpression in these cells does not appear to be related to cell cycle progression. Another activity of NEK6 that has been implicated in its oncogenic activity is inhibition of p53-mediated senescence (Jee *et al*., 2010). LHSR-AR cells express large-T antigen, so the p53 pathway should be inactive in these cells. To confirm this in our multiply infected LHSR-AR cells, they were exposed to etoposide at 10 μM for 18 hours or 50 μM for 4 hours: under neither condition is p21 expression induced, while the level of cleaved PARP is not altered by NEK6 expression (Supplemental Figure 4C). Thus NEK6 does not act by modulating the p53 pathway, and furthermore the pro-survival effect of NEK6 appears to be specific to the *in vivo* context of castration resistance.

Milestones 2 and 3: NEK6 does not activate AR signaling and does not lead to detectable STAT3 phosphorylation in LHSR-AR cells. In addition, there is no evidence that NEK6 activates beta-catenin or RPS6KB1 signaling, promotes cell cycle progression, or antagonizes p53 signaling in our model.

Milestone 4: Generation of mRNA and phosphoproteomic signatures corresponding to androgen independence conferred by our hits, and comparison to androgen signaling and existing databases

Identification of FOXJ2, NCOA5, CSNK1A1 and YES1 as NEK6 substrates

To gain a more comprehensive understanding of the immediate signaling mediated by NEK6 expression and discover novel *in vivo* substrates, we performed a phosphoproteomic analysis. Constructs for the expression of wild-type and kinase-dead NEK6 under the control of a doxycycline-inducible promoter were introduced into LHSR-AR cells, and we created phosphoproteomic profiles of cells expressing doxycycline inducible versions of: (1) wild-type NEK6 in the presence of doxycycline, (2) kinase-dead NEK6 in the presence of doxycycline, and (3) wild type NEK6 without doxycycline. Cells were cultured in “light”, “medium”, and “heavy” media for Stable Isotope Labeling by Amino acids in Cell culture (SILAC) for 7 days in 2 different permutations; they were growth factor starved for the final 30 hours and then growth factor stimulated for 5 minutes. Lysates were then subjected to SCX-IMAC phosphorylation analysis and assayed by mass spectrometry.

A total of 9418 phosphopeptides (8432 phosphoserine, 952 phosphothreonine, 34 phosphotyrosine) from 3401 proteins were detected in this experiment. 59 phosphopeptides from 50 proteins were increased in both the wild-type induced vs. un-induced and wild-type vs. kinase dead comparison with a combined q value of <0.25 (Supplemental Table 2). The differentially phosphorylated proteins include a large number of transcriptional regulators, including the forkhead-box family proteins FOXO3 and FOXA1, and the phosphopeptides represent a variety of common phophorylation motifs as shown in Table 2. Among these motifs are pS/pT-P, associated with MAPK/CDK/GSK3 signaling, and R-X-R-X-X-pS/pT, associated with AKT and RSK (ribosomal S6-kinase) signaling. We noted that the frequency of these motifs among the 59 differential phosphopeptides is not increased as compared to their frequency among all detected phosphopeptides - for example, pS/pT-P motifs were found in 26 of the 59 differential phosphopeptides vs. 4815 of the 9434 total phosphopeptides (44% vs. 51%, p=NS). This suggests that NEK6 does not globally activate MAPK/CDK/GSK3, AKT/RSK, CAMK or CK2 signaling.

However, a canonical NEK6 motif (Vaz Meirelles *et al*., 2010) with leucine at the -3 position [L-X-X-pS/pT-F/W/Y/M/L/I/V/R/K] is more frequently represented in the 59 significantly enriched phosphopeptides compared to all detected phosphopeptides (p=0.0092 Fisher’s exact); an “acceptable” NEK6 substrate motif [L/F/W/Y-X-X-pS/pT-F/W/Y/M/L/I/V/R/K] is even more significantly enriched ($p=1.95\times10^{-5}$). This suggests that this peptide sequence is a true description of the NEK6 phosphorylation motif, and that the 8 proteins with phosphopeptides of this form detected here

(FOXJ2, HUWE1, NCOA5, KRT18, TRA2B, HNRNPM, HNRNPA2B1, ZNF326) are bona fide *in vivo* NEK6 substrates.

Table 2. Summary of phosphoproteomic data

	L-X-X-pS/pT-F/W/Y/M/L/I/V/R/K (NEK6 general consensus)	L/F/W/Y-X-X-pS/pT-F/W/Y/M/L/I/V/R/K (NEK6 acceptable)	pS/pT-P (proline-directed kinases)	R-X-R-X-X-pS/pT (AKT1 or RSK family)	R-X-X-pS/pT (CaMK consensus)	pS/pT-D/E-X-D/E (CK2 consensus)	Others
Proteins with phosphopeptides meeting significance threshold (59 total phosphopeptides representing 50 proteins)	FOXJ2 HUWE1 NCOA5 KRT18	FOXJ2 HUWE1 NCOA5 KRT18 TRA2B (Y-X-X-pS-Y) HNRNPM (F-X-X-pS-F) HNRNPA2B1 (F-X-X-pS-F) ZNF326 (F-X-X-pS-Y)	FOXO3 TRPS1 LMO7 SATB2 PAK6 BCL6 FOXA1 KLF4 ATXN1 IRF2BP1 RFX2 HIVEP2 KLF3 Others (×13)	SLC2A12 FAM21C ATXN1	SLC2A12 FAM21C ATXN1 ATM LMO7 DROSHA PLEKHA6 RIPK3 MYOF EXPH5 MLLT3	ERCC5 LIG1 PBRM1	16 phosphopeptides representing 14 proteins 12 pS 3 pT 1 pY
Enrichment (compared to all detected phosphopeptides)[a]	4/59 vs. 131/9362 (p=0.0092 Fisher's exact)	8/59 vs. 186/9362 ($p=1.95\times10^{-5}$)	26/59 vs. 4815/9434 (p=NS)	3/59 vs. 434/9301 (p=NS)	11/59 vs. 2239/9362 (p=NS)	3/59 vs. 701/9417 (p=NS)	

[a] The denominator for the total number of detected phosphopeptides in each column is filtered for only those phosphopeptides able to be defined as representing this motif (i.e. only those phosphopeptides where the -5 amino acid was detected by mass spectrometry were assessed for representing the AKT/RSK motif)

To confirm whether detection of these phosphopeptides in cells is due to direct phosphorylation by NEK6, we assessed the activity of commercially available recombinant GST-NEK6 on a subset of these proteins immunoprecipitated via a C-terminal V5-tag through an on-bead kinase assay. We initially focused on the transcription factors FOXJ2 and NCOA5 because they are related to families of transcription factors already described to be important in prostate cancer (Tao, *et al*., 2014; Qin *et al*., 2014). We were able to confirm phosphorylation of FOXJ2 and NCOA5, with no phosphorylation of a lacZ control (Figure 5A). Mutation of the phosphorylation sites of FOXJ2 and NCOA5 identified via mass spectrometry, Ser8 and Ser96 respectively, decreases the *in vitro* phosphorylation of these substrates, demonstrating the specificity of the kinase activity at these residues.

To expand our phosphoproteomic studies *in vivo* we sought to elucidate NEK6-interacting proteins and potential substrates in the tumors themselves. To identify *in vivo* interacting proteins using mass spectrometry, we analyzed tumors that formed in female mice from LHSR-AR cells overexpressing a form of NEK6 with a C-terminal V5 tag or overexpressing untagged NEK6; protein lysates from these tumors were subjected to immunoprecipitation with anti-V5 magnetic beads. Proteins enriched in the immunoprecipitate from NEK6-V5 expressing tumors compared to tumors expressing NEK6 without a V5-tag (from which the immunoprecipitate would consist only of proteins bound non-specifically to the beads) were considered as candidate *in vivo* interacting proteins. A total of 258 proteins were identified that were enriched with a $\log_2$ ratio of greater than 1.25 in the experimental sample vs. the control (Supplemental Figure 3). Gene Ontology (GO) terms associated with this set of proteins as determined through the Gene Ontology for Functional Analysis (GOFFA) software (Sun *et al*., 2006) are listed in Table 3.

From this list, we focused on the interacting protein kinases, as direct substrates of NEK6 that are protein kinases would likely mediate further signaling downstream from NEK6 overexpression. We obtained ORFs for nine of the interacting proteins identified in this analysis and then performed an *in vitro* kinase assay with NEK6. As seen in Figure 5A, NEK6 potently phosphorylates the kinases CSNK1A1 and YES1 *in vitro*.

Table 3. NEK6-interacting proteins from tumors categorized by GO term

Cytoskeleton		Nucleoside triphosphatase activity		Calcium ion binding	Signal transduction		Protein kinase	Nucleotide metabolic process	Misc.
ACTC1	MYH9	ACTC1	MYO1D	ACTN4	ALDH1A1	NPM1	CAD	ACTC1	***Ribosome***
ACTN4	MYL12B	ATAD3B	MYO1E	AIF1L	ANXA1 (CALM1)	PHB	CAMK2D	ALDH1A1	GNB2L1
ACTR1A	MYL6	ATL3	MYO5A	ANXA1	CAMK2D	PPP2R2A	CPNE3	ATL3	RPL10A
ACTR2	MYL9	ATP1A1	MYO5C	ANXA2 (CALM1)	CDC37	PRDX4	CSNK1A1	ATP1A1	RPL14
ACTR3	MYO18A	ATP5C1	MYO6	CALML3	CLTA	PSMC1	CSNK2B	ATP1A4	RPL18
AIF1L	MYO1B	ATP5O	PSMC1	GSN	CNGB1	PSMC5	IKBKB	ATP5C1	RPL18A
ALDOC	MYO1D	DCTN1	PSMC5	MYL12B	CSNK1A1	PSMC6	MAP2K2	ATP5O	RPL27
ANXA1	MYO1E	DDX3X	PSMC6	MYL6	CSNK2B	PSMD1	MAPK1	CAD	RPL4
ARPC1A	MYO5A	EEF1A1	RAB11B	MYL9	CTNND1	PSMD14	NEK6	CNP	RPL7A
ARPC2	MYO5C	EEF2	RAB14	PLS3	DDB1	RAB11B	NEK7	CTPS	RPS15A
ARPC4	MYO6	EIF4A1	RAB35	S100A10	DOCK7	RAB14	NEK9	DOCK7	RPS25
ARPC5	NPM1	EIF4A3	RAB5A	S100A11	DPYSL2	RAB1B	NME2	FLNA	RPS27
ARPC5L (CALM1)	PDCD6IP	GNA13	RAB7A	S100A2	FLNA	RAB35	PRKDC	GNA13	RPS3
CAPZA1	PDLIM1	GNB1	RAN	S100A4	FLNB	RAB5A	RPS6KA1	GNB1	RPS3A
CAPZB	PDLIM5	GNB2	RHOC	S100A8	GMFB	RAB7A	RPS6KA3	GNB2	RPS4X
CCT3	POTEKP	HSP90AA1	RRAS2	S100A9	GNA13	RAN	TWF1	GNB2L1	RPS5
CCT4	RAI14	HSPA8	RUVBL1	SLC25A13	GNB1	RHOC	YES1	HSP90AA1	UBA52
CCT5	RCC2	KIF21B	RUVBL2	SSR4	GNB2	RPS6KA1		IQGAP1	***Proteasomal complex***
CDK5RAP2	RUVBL1	KIF5B	SETX	TPM4	GNB2L1	RPS6KA3		MYH9	PSMC1
CEP350	S100A8	KRAS	TUBA1C		GSN	RRAS2		NAMPT	PSMC5
CNN2	S100A9	MCM5	TUBB		GSTP1	S100A10		NME2	PSMC6
CORO1A	SEPT2	MYH10	TUBB2A		HNRNPK	S100A11		NPPC	PSMD1
CORO1B	SPRR1B	MYH14	TUBB2C		HSP90AA1	S100A4		PSMC1	PSMD14
CSNK1A1	SPTBN2	MYH9	TUBB6		IKBKB	S100A9		PSMC5	VCP
CTTN	SVIL	MYL6	TUFM		IQGAP1	SFN		PSMC6	
DBT	TCP1	MYO18A	VCP		KRAS	TOLLIP		RAB11B	***Unfolded protein binding***
DCTN1	TMOD1	MYO1B	YME1L1		KRT18	UACA		RAB14	CALR
DSTN	TMOD3				MAP2K2	UBA52		RAB35	CCT3
FLNA	TPM1				MAPK1	VAPA		RAB5A	CDC37
FLNB	TPM4				MYH9	VCP		RAB7A	DNAJA2
GNB2L1	TUBA1C				MYO1E	YWHAE		RAN	DNAJA4
GSN	TUBB				MYO6	YWHAG		REXO2	HSP90AA1
IQGAP1	TUBB2A				NAMPT	YWHAH		RHOC	HSPA2
KIF21B	TUBB2C				NEK6	YWHAZ		RRAS2	HSPA9
KIF5B	TUBB6							RUVBL2	NAP1L4
KRT18	TWF1							SLC25A13	PPIA
KRT8	UACA							SULT2B1	PPIB
LIMA1	YWHAE							TPI1	
MYH10	YWHAZ							TPM1	
MYH14	ZNF185							VCP	
								XDH	

While the two approaches of *in vitro* phosphoproteomic analysis using SILAC and *in vivo* interactomic analysis can identify a large number of putative substrates, neither approach is comprehensive due to limitations of the detection platforms. Thus, we sought to validate and determine the biological consequences of NEK6 phosphorylation of the top candidates identified through both approaches.

Mapping NEK6 phosphorylation sites on FOXJ2, NCOA5, CSNK1A1 and YES1

To comprehensively map the phosphorylation sites of NEK6 on FOXJ2, NCOA5, CSNK1A1 and YES1, all serine and threonine residues in these proteins in "acceptable" NEK6 phosphorylation motifs as described above [L/F/W/Y-X-X-pS/pT-F/W/Y/M/L/I/V/R/K] were identified; when the relevant serines and threonines are mutated to aspartic acid, the resulting mutant forms of these proteins are phosphorylated significantly less than the wild type counterpart (compare lanes 2 and 1 in right panels of Figures 5B and C, and Figures 6B and C). When mutating all of these potential phosphorylation sites but maintaining one of the serines/threonines as wild type, it is apparent that NEK6 can phosphorylate FOXJ2 at Thr23 and Ser254 (Figure 5B, lanes 3 and 5) in addition to Ser8; NCOA5 at Ser21 and Ser151 (Figure 5C, lanes 3 and 4) in addition to Ser96; CSNK1A1 at Ser96, Thr129, and Thr287 (Figure 6B, lanes 4-6) and YES1 at Thr295 and Ser524 (Figure 6C, lanes 5-6).

Gene Expression changes mediated by NEK6

To further elucidate downstream signaling mediated by NEK6 overexpression, we sought to determine gene expression changes in tumors with NEK6 overexpression in castrate conditions. We established tumors at 3 subcutaneous sites of male mice implanted with a testosterone pellet from cells expressing NEK6 under a doxycycline-inducible promoter. After tumors were formed, doxycycline was withdrawn from half the mice 7 days prior to planned tumor harvest. Mice were then castrated and testosterone pellets removed; they were then sacrificed and tumors were harvested at days 0, 2 and 5 after castration. As seen in Figure 7A, withdrawal of doxycycline reduces NEK6 levels to near the levels in tumors without exogenous NEK6 expression. Messenger RNA was then isolated from tumors from the day 2 and day 5 time points and subjected to gene expression analysis using RNASeq.

Gene expression changes with NEK6 overexpression in tumors at day 5 after castration demonstrate some overlap with upregulated and downregulated genes in the comparison of NEK6 wild-type vs. kinase-dead overexpression in LHSR-AR cells *in vitro* in the experiment described in Supplemental Figure 1D (Figure 7B). Given that the gene expression was measured in different contexts (tumors vs. culture) and using different assays (RNASeq vs. Affymetrix microarray) in both comparisons, the genes in this overlap are high confidence NEK6 downstream transcriptional targets. Interestingly, the upregulated genes include prostate stem cell antigen (PSCA), which is a marker of late intermediate prostate epithelial cells (Tran *et al*., 2003) that has been reported to be increased in prostate cancer metastasis (Lam, *et al*. 2005); and keratin 13 (KRT13), which is a marker of squamous differentiation in the pathology literature (van Dorst *et al*, 1998).

To further characterize these gene expression changes, Gene Set Enrichment Analysis was performed on the signature derived from tumors overexpressing NEK6 at day 5 after castration compared to controls (Figure 7C). The top two curated gene sets (C2) from the molecular signatures database (MSigDB) correlated with the NEK6 signature are 1) genes down-regulated in primary B lymphocytes within 60-180 min after activation of LMP1, an oncogene encoded by Epstein-Barr virus (Dirmeier *et al*, 2005) and 2) genes representing the epithelial differentiation module in sputum during asthma exacerbations (Bosco, *et al*., 2010). GOFFA reveals the most statistically significant GO biological process associated with NEK6 upregulated genes to be "response to biotic stimulus" (p=0.0005); other relevant terms include "type I interferon signaling pathway" (p=0.0023), "apoptotic signaling pathway" (p=0.0056), "cytoskeleton organization" (p=0.0084) and "epithelial cell differentiation" (p=0.0183). More broadly, 68 NEK6 upregulated genes are categorized under "developmental process," and 33 genes are categorized under "immune system process," so we used these GO terms as a framework for subsequent assessments of gene expression changes in tumors.

We hypothesized that NEK6 could mediate resistance to castration in tumors by maintaining survival signaling that is lost when AR is no longer activated by circulating androgens. To understand components of this survival signaling, we compared gene expression of control tumors (i.e. without NEK6 overexpression) at the day 2 and day 5 time points. Using gene set enrichment analysis (GSEA) we find that the top gene set and five of the top 10 gene sets associated with gene expression lost following castration reflect interferon signaling (Table 4, Figure 8A left). This suggests that in our *in vivo* model, much of the survival signaling mediated by circulating androgens involves expression of genes associated with these pathways. Interferon-related gene sets have previously been described as being biologically important in prostate cancer, particularly with regards to differences in signaling between cancers in patients with African and European ancestry (Wallace *et al*., 2008 – Figure 8A, right) and in treatment resistance (Weichselbaum, *et al*., 2008; Cheon *et al*., 2013).

Table 4. Gene sets enriched in ranked list of genes with decreased expression after castration (Control Day 5 vs. Day 2)

	GS	SIZE	ES	NES	NOM p-val	FDR q-val	FWER p-val
1	REACTOME_INTERFERON_ALPHA_BETA_SIGNALING	46	0.69	3.2	0	0	0
2	LIANG_SILENCED_BY_METHYLATION_2	44	0.64	3.04	0	0	0.001
3	BOWIE_RESPONSE_TO_TAMOXIFEN	17	0.82	3	0	0.001	0.003
4	BROWNE_INTERFERON_RESPONSIVE_GENES	61	0.6	2.98	0	0.001	0.005
5	ZHANG_INTERFERON_RESPONSE	20	0.78	2.98	0	0.001	0.005
6	BOWIE_RESPONSE_TO_EXTRACELLULAR_MATRIX	16	0.8	2.97	0	0.001	0.009
7	MOSERLE_IFNA_RESPONSE	30	0.68	2.93	0	0.002	0.013
8	SANA_TNF_SIGNALING_UP	71	0.56	2.92	0	0.002	0.016
9	LIU_VAV3_PROSTATE_CARCINOGENESIS_UP	59	0.57	2.88	0	0.003	0.023
10	DER_IFN_ALPHA_RESPONSE_UP	69	0.55	2.88	0	0.002	0.023

Gene Expression changes mediated by NEK6 substrates

In order to determine the role of the identified substrates in mediating signaling downstream of NEK6, we assess signaling in tumors mediated by phosphomimic forms of these substrates with serine to aspartic acid substitutions of the phosphorylation sites identified *in vitro*. These phosphomimic forms were not sufficient either alone or in combination to generate castration-resistant tumors (data not shown). In order to interrogate downstream signaling mediated by these substrates in castration-resistant tumors, we expressed them under a doxycycline-inducible promoter in tumors formed in male mice, which were harvested for RNASeq five days after castration from mice with continued doxycycline treatment or 7 day doxycycline withdrawal as for NEK6 previously. GSEA reveals that the gene expression changes mediated by phosphomimic forms of CK1α, FOXJ2, and YES1, but not NCOA5, are statistically significantly correlated with the NEK6 signature. These correlations are not due to technical artifact or systemic bias in the tumor samples with continued expression of the transgene (+dox) vs. discontinuation of expression (-dox) because 1) the genes upregulated by expression of phosphomimic forms of FOXJ2, CK1α and YES1 are largely non-overlapping 2) a transgene assayed in the same system, NCOA5, does not demonstrate statistically significant overlap and 3) when performing comparative marker selection for all +dox samples vs. the –dox samples, no gene is upregulated in the comparison with a signal to noise ratio greater than 1.

The phosphomimic substrate with the highest degree of correlation with the NEK6 signature is CK1α (Figure 8C). The set of genes that are upregulated by both CK1α(3S→D) and NEK6 is highly enriched for genes involved in developmental processes (the top GO biological process with >3 genes in the overlap is “epithelial cell differentiation” p=0.0012). Included in this overlap is KRT13, a marker of squamous differentiation, suggesting that CK1α is involved in the transdifferentiation of NEK6-mediated castration resistant tumors to a squamous phenotype. In addition, RNASeq suggests that FOXJ2 is the relevant transcription factor for some of the high confidence NEK6 transcriptional targets (TPPP3, PSCA, PLAC8) from Figure 7B, and that YES1 is also involved in aspects of the differentiation phenotype (Supplemental Figure 5).

As mentioned previously, transduction of LHSR-AR cells with a combination of phosphomimic forms of the identified substrates is not sufficient to lead to androgen-independent tumor formation. Interestingly, none of these phosphomimics leads to much upregulation of “immune response” genes, and we hypothesize that this signaling may be important for the castration resistance phenotype, particularly since the genes downregulated by castration in this model are highly correlated with interferon/TNF signaling. The NEK6 interactome as shown in Table 3 includes many genes putatively involved in immune signaling including IKBKB, DDX3X, ILF2, PRDX4, RHOC, S100A8, S100A9, and TOLLIP; however, none of these proteins act as direct NEK6 substrates *in vitro* in comparison to the potent substrates CK1α and YES1 (Supplemental Figure 6). In addition, NEK6 has previously been reported to interact with RELB (Vaz

Meirelles *et al*., 2010) and increase the activity of an NFκB promoter (Matsuda *et al*., 2003), and it has also been previously reported to phosphorylate STAT3 (Jeon *et al*., 2010); however, RELA, RELB, STAT1, STAT3, and STAT5 are also not phosphorylated to an appreciable extent by NEK6 in our *in vitro* kinase assay. Thus, the impact of NEK6 on immune signaling may be indirect or the relevant substrate(s) have yet to be identified.

Milestone 4: Phosphoproteomic studies reveal novel substrates FOXJ2, HUWE1, NCOA5, KRT18, TRA2B, HNRNPM, HNRNPA2B1, ZNF326. Proteomic studies identify a number of potential interacting proteins in tumors; of these CSNK1A1 and YES1 are also *in vitro* substrates. Gene expression studies reveal NEK6 likely mediates castration resistance through alteration of cell differentiation state and maintenance of immune-related signaling that is normally lost with castration.

Milestone 5: Determine evidence for NEK6 and NLK conferring castrate resistance in clinical samples and identify subsets of patients displaying genomic changes and expression signatures corresponding to resistance mediated through the activity of a particular gene/pathway.

NEK6 is overexpressed in several malignant tissues and cell lines, and has been previously been implicated in cell transformation (Jeon *et al*., 2010; Nassirpour *et al*., 2010; Wang *et al*., 2014). Cancer types previously described to have high frequency of NEK6 overexpression include cancers of the liver (Chen *et al*., 2006; Jeon, *et al*., 2010; Cao, *et al*., 2012), stomach (Takeno, *et al*., 2008; Nassirpour *et al*., 2010), breast (Jeon *et al*., 2010; Nassirpour *et al*., 2010), uterus, colon/rectum and ovary (Nassirpour *et al*., 2010). In human prostate cancer, the NEK6 locus at chromosome 9q33.3 is present in a region of low level copy number gain (Taylor *et al*., 2010; Huang *et al*., 2012; Grasso *et al*., 2012) without a known validated prostate cancer oncogene. Genomic characterization of human prostate cancers through the Prostate TCGA and SU2C-PCF Dream Team efforts demonstrates amplification or mRNA overexpression (z-score>2) of NEK6 in 7% of primary tumors and 6% of metastases (www.cbioportal.org/prostate-portal/).

We performed immunohistochemistry analysis of primary prostate cancers compiled in seven tumor microarrays (TMA) generated by the Gelb Center for Translation Research at Dana-Farber Cancer Institute using an antibody we optimized for IHC (Supplemental Figure 2A and B). NEK6 expression was quantified by spectral imaging. We failed to find detectable levels of NEK6 protein in most prostate tissues, but found that NEK6 is aberrantly expressed in ~16% of tumors (Supplemental Figure 2C). NEK6 expression was greater in tumor samples than in benign-appearing glandular epithelium from these same radical prostatectomy specimens (one-tailed p=0.0012 by Student's T-test), suggesting that NEK6 expression is associated with tumor progression (Figure 3A). We are in the process of correlating NEK6 status with grade and outcomes based on the schema in Figure 3B.

It remains unclear at this point whether *de novo* acquisition of NEK6 amplification or overexpression is a mechanism of development of castration resistance in advanced prostate cancer. The strongest evidence for this would be detection of markers of overactive NEK6 signaling in metastatic CRPC in comparison to therapy-naïve samples, which per our model would be most likely to be detected in prostate cancers that have become AR-independent. A recent study by Grasso *et al* (2012) genetically profiled 35 cases of CRPC in comparison to 59 cases of localized PrCa. The primary difference in the genomic landscape in these two states was massive amplification of the AR in CRPC in comparison to the primary cases; there was no increase in amplitude of the region of copy number gain on 9q33.3 where NEK6 is located. There was no evidence for enrichment in genetic markers of any other signaling pathways in CRPC cases, though this is likely due to the fact that these cases were collected at a time when many of the current novel hormonal therapies had not yet been in widespread use. Efforts to genetically characterize larger numbers of CRPC cases, including those from patients who have progressed on novel hormonal therapies, are currently underway at DFCI (http://www.aacr.org/home/public--media/stand-up-to-cancer/su2c-dream-teams/su2c-pcf-dream-team-precision-therapy-of-advanced-prostate-cancer.aspx).

We analyzed the levels of NEK6 expression in several patient-derived prostate cell lines by immunoblotting (Figure 4A) and found that most prostate cancer cell lines expressed higher levels of NEK6 than immortalized (RWPE, PrEC-LH) and transformed (LHSR-AR) prostate epithelial cells. Interestingly, NEK6 levels were relatively high in VCaP and LNCaP cells, suggesting that high expression of NEK6 was not sufficient to overcome the *in vitro* androgen dependence of these cells; however, it is important to note that these cells were derived from patients with castration resistant disease *in vivo*. To test whether NEK6 was essential for *in vitro* proliferation of androgen-independent AR-low cell lines (reminiscent of the AR-low xenograft tumors), we introduced doxycycline-inducible shRNAs targeting NEK6 to CL-1, PC-3 and DU145 cells (Figure 4B). Despite near complete suppression of NEK6 expression, there was no effect on

proliferation of the cell lines except a modest suppression of DU145 proliferation with shRNA#2. These observations are in consonance with a prior report suggesting that NEK6 is not essential for proliferation of many mammalian cell lines (Nassirpour, *et al*., 2010).

Milestone 5: NEK6 is aberrantly expressed in a subset of primary human prostate cancer. Efforts to characterize metastatic biopsies from patients with CRPC for sequencing and assessing gene expression are underway.

Task 9: Genome wide screen of genes conferring androgen-independence to androgen-dependent cell line

Milestone 6: Identify a set of genes leading to androgen-independent prostate cancer cell growth in vitro and in vivo.

To ensure adequate representation of each gene in the kinome library in our original *in vivo* functional genomic screen, we implanted mice with LHSR-AR cells transduced with 9-10 ORF constructs in each pool. It would be impractical to expand this screen to a genome-wide library because of the number of mice and amount of material, time and effort required. In order to obtain a more manageable list of genes to query in our *in vivo* assay, we first aim to identify genes that can confer androgen-independent proliferation to the androgen-dependent LNCaP prostate cancer cell line *in vitro*. This experiment will be performed as a pooled screen using a barcoded lentivirally-delivered library encompassing ~20,000 ORFs available through the Broad Institute Genetic Perturbation Platform using the schema in Figure 9. The cells will be infected at a target infection rate of 30% to achieve a multiplicity of infection (MOI) of 1 and target representation of 1000 cells infected with each ORF. The representation of ORFs at each time point will be assessed by isolating genomic DNA, performing targeted sequencing of the barcodes, and deconvoluting enriched ORFs as represented by their correnspondingbarcodes. ORF representation will be assessed at an early time point and after 7 weeks of selection, either in media with androgen-poor charcoal stripped serum (CSS) or media+CSS+2.5 uM enzalutamide, both compared with cells grown in androgen-containing media with fetal bovine serum (FBS) as a control. Three replicates will be obtained for each condition, and candidates identified through the screen will be validated in low throughput, and also assessed *in vivo* for conferring androgen independent xenograft tumor formation to LHSR-AR cells and enzalutamide resistance to xenografts derived from LNCaP cells overexpressing the androgen receptor (LNCaP-AR cells).

Conditions for achieving infection rate of 30% have been defined, and we will initiate the screen over the next few weeks.

KEY RESEARCH ACCOMPLISHMENTS

- Identification of NEK6 as a novel mediator of castration resistance in an *in vivo* forward functional genomic screen.
- Demonstration that kinase activity and continued expression of NEK6 is required for maintenance of castration resistance, suggesting its suitability as a therapeutic target.
- Discovery of novel NEK6 substrates FOXJ2, HUWE1, NCOA5, KRT18, TRA2B, HNRNPM, HNRNPA2B1, ZNF326 in cell culture.
- Isolation of an *in vivo* NEK6 protein complex that contains two kinases, CSNK1A1 and YES1, which are also *in vitro* substrates of NEK6.
- Determination that NEK6 overexpression in tumors leads to maintenance of immune-related signaling normally lost with castration, as well as squamous transdifferentiation
- Demonstration that NEK6 substrates FOXJ2, CSNK1A1 and YES1 mediate a subset of the gene expression changes induced by NEK6 overexpression, with CSNK1A1 most closely related to the squamous differentiation phenotype
- Determination that NEK6 is aberrantly expressed in subset of human prostate cancer
- Optimization of a genome-wide barcoded ORF screen of genes conferring androgen independent proliferation of LNCaP cells in vitro

REPORTABLE OUTCOMES

Research Investigations
Atish D. Choudhury[1,2,3], Jane Lock[1], Isil Guney[1], Ted Pei[1], Anna C. Schinzel[1,3], Francesca Izzo[1,3], Rosina Lis[1,4,] Maura Cotter[1], Michaela Bowden[1], Mari Nakabayashi[1], Lillian Werner[1], Matthew Chabot[1], Yvonne Y. Li[1], Jenn Abelin[3], Jinal Patel[3], Christina Hartigan[3], Gaelen Guzman[3], Emily Hartman[3], Monica Schenone Tchernychev[3], Jacob D. Jaffe[3], Philip W. Kantoff[1,2], Massimo Loda[1,2,3,4], Peter S. Hammerman[1,2,3], William C. Hahn[1,2,3].
NEK6 mediates castration resistance in prostate cancer in vivo (manuscript in progress)

Reviews
Choudhury AD, Eeles R, Freedland SJ, Isaacs WB, Pomerantz MM, Schalken JA, Tammela TL, Visakorpi T. "The role of genetic markers in the management of prostate cancer." *Eur Urol.* 2012 Oct;62(4):577-87.

Choudhury AD, Kantoff PW. "New Agents in Metastatic Prostate Cancer". *J Natl Compr Canc Netw.* 2012 Nov 1;10(11):1403-9.

Abstracts, Poster Presentations and Exhibits Presented at Professional Meetings

Invited Presentation

Regional

2015 "NEK6 as a Novel Mediator of Castration Resistance in Prostate Cancer." RNAi/ MicroRNAs & Stem Cells (GeneExpression Systems), May 4, 2015, Cambridge MA.

2015 "Molecular Characterization of Circulating Tumor Cells in Prostate Cancer" ToPCaP Junior Investigators seminar. April 30, 2015, Boston MA.

2014 "Genetic Characterization and Analysis of CTCs in Clinical Practice." Circulate Symposium (Hanson Wade), November 20, 2014, Boston MA.

National

2014 "What, when and to whom? Controversies in systemic treatment of prostate cancer." Tatar Family Foundation Cancer Symposium. September 10, 2014, Dayton OH.

2013 "Functional and Genomic Characterization of Viable CTCs enabled by nanowells." 20th Annual Prostate Cancer Foundation Scientific Retreat. October 25, 2013. High achieving Young Investigator presentation.

2011 "Molecular Determinants of Hormone Refractory Prostate Cancer." 18th Annual Prostate Cancer Foundation Scientific Retreat, September 21, 2011, Young Investigator presentation.

Poster Presentations
Choudhury AD, Lock J, Guney I, Pei T, Schinzel AC, Izzo F, Lis RT, Stack EC, Nakabayashi M, Werner L, Petrozziello G, Chabot M, Abelin J, Patel J, Jaffe JD, Kantoff PW, Loda M, Hahn WC. "An *in vivo* functional genomic screen identifies NEK6 as a novel mediator of castration resistance in prostate cancer." 7th Annual Multi-institutional Prostate Cancer Program Retreat, March 16-18, 2014. Poster selected for presentation.

Choudhury AD, Lohr JG, Adalsteinsson VA, Yao X, Cibulskis K, Rosenberg M, Sougnez C, Nakabayashi M, Lis RT, Lee GM, Li T, Chabot MS, Ly A, Taplin ME, Loda M, Kantoff PW, Golub TR, Wittrup KD, Getz G, Boehm JS, Love JC. "Functional and Genomic Characterization of Viable CTCs enabled by nanowells." Dana-Farber Cancer Institute Molecular and Cellular Oncology Department Retreat. January 27, 2014. 1st place winner.

Choudhury AD, Lohr JG, Adalsteinsson VA, Yao X, Cibulskis K, Rosenberg M, Sougnez C, Nakabayashi M, Lis RT, Lee GM, Li T, Chabot MS, Ly A, Taplin ME, Loda M, Kantoff PW, Golub TR, Wittrup KD, Getz G, Boehm JS, Love JC.

"Functional and Genomic Characterization of Viable CTCs enabled by nanowells." Prostate Cancer Foundation 20th Annual Scientific Retreat. October 24-26, 2013.

Choudhury AD, Guney I, Schinzel AC, Izzo F, Stack EC, Nakabayashi M, Petrozziello G, Hahn WC. "Molecular Determinants of Hormone Refractory Prostate Cancer." 5th Annual Multi-institutional Prostate Cancer Program Retreat, March 19-21, 2012. Poster selected for presentation and awarded as a prize winner.

Choudhury AD, Guney I, Schinzel AC, Izzo F, Stack EC, Nakabayashi M, Petrozziello G, Hahn WC. "Molecular Determinants of Hormone Refractory Prostate Cancer." Dana-Farber Cancer Institute Molecular and Cellular Oncology Department Retreat. April 9, 2012.

CONCLUSIONS

We have performed an unbiased *in vivo* functional genomic screen to identify kinases that can confer androgen independence in a model of androgen-dependent prostate tumor formation, and discovered NEK6 as a novel mediator of castration resistance. The NEK6 gene on 9q33.3 is located on a region of recurrent copy number gain in prostate cancer, and it is overexpressed in a subset of primary human prostate cancers and most patient-derived prostate cancer cell lines tested. We are unable to correlate protein expression to amplification of the locus or mRNA overexpression in these samples, so it is unknown whether aberrant NEK6 protein expression is driven by genetic/transcriptional changes vs. other translational or post-translational determinants of protein levels. NEK6 plays a mechanistic role in the development of castration resistance in our model, and turning off its expression in xenograft tumors where it is overexpressed restores sensitivity to castration, suggesting that its continued activity is required for tumor maintenance in this context. The finding that NEK6 is not essential for mammalian cells, along with the fact that mice homozygous for a targeted null NEK6 allele (**Nek6^{tm1Dgen}**) demonstrate no apparent phenotype (https://www.infrafrontier.eu/sites/infrafrontier.eu/files/upload/public/deltagen/DELTAGEN_T518/) except for promotion of cardiac hypertrophy induced by transthoracic aorta constriction (Bian *et al*., 2014), suggests that NEK6 could be safely therapeutically targeted in prostate cancer and other cancer types where it is a relevant driver without a high degree of systemic toxicity.

The role of NEK6 in oncogenic signaling have been proposed to be mediated by cell cycle progression/cyclin B modulation (Zhang *et al*., 2014), inhibition of p53-mediated senescence (Jee *et al*., 2010), phosphorylation of STAT3 (Jeon *et al*., 2010), and blocking nuclear translocation of SMAD4 to antagonize TGFβ signaling (Zuo *et al*., 2014). However, there is little evidence from our unbiased studies suggesting any of these pathways as the predominant mechanism of NEK6-mediated castration resistance in our model. Previous proteomic work (Vaz Meirelles *et al*., 2010) identifies multiple interacting partners and substrates that implicate NEK6 in a variety of signaling pathways including cell cycle, cytoskeleton organization, DNA repair, Notch and NFκB pathways. In our studies, the gene expression signature mediated by NEK6 overexpression in the context of castration implicates differentiation and immune processes in conferring castration resistance to tumors. Analysis of gene expression changes induced by phosphomimic forms of newly identified substrates FOXJ2, NCOA5, CK1α and YES1 reveals elements of NEK6 signaling likely mediated by these proteins. In particular, the gene expression profile generated through expression of a phosphomimic form of CK1α highly correlates with the NEK6 signature, particularly with regards to markers of squamous differentiation. CK1α has previously been implicated in Wnt-β-catenin signaling in cancer (Cruciat, 2014), but this does not appear to be the operant mechanism of action in our system given that there is no evidence for nuclear β-catenin in the xenograft tumors by IHC and no evidence for upregulation of a β-catenin signature by RNASeq/GSEA. Recent studies suggest CK1α as a potential therapeutic target in acute myeloid leukemia (Järås *et al*., 2014), 5q- myelodysplastic syndrome (Schneider *et al*., 2014), and multiple myeloma (Hu *et al*., 2015), and our current studies would suggest NEK6/CK1α signaling as a possible therapeutic target in certain forms of castration-resistant prostate cancer. However, given that the substrates identified here are not sufficient to confer castration resistance, there are likely other substrates important to the phenotype that we have yet to characterize (including, for example, the other 6 putative substrates identified in the *in vitro* phosphoproteomic screen).

Parallel growth factor signaling has been implicated in androgen independence in several model systems, but this phenotype depends on both the growth factor milieu of the microenvironment and the underlying genetic context of the cancer cells with regards to their behavior in this milieu. The use of engineered cell lines allows control over the genetic context, and the use of xenografts allows testing different *in vivo* environments where the limiting nutrients and growth factors are unknown and thus could not be replicated in a culture environment. While NEK6 is a potent mediator of

castration resistance in this model, it is reasonable to consider that other genes might be identified to confer androgen independence in different genetic contexts in different microenvironments.

While alterations in the AR gene and in AR-mediated signaling have already been demonstrated to play a role in the development of castration resistance (Sharifi, 2013), it is apparent that resistance to hormonal therapies can arise through progression to states where the androgen receptor is no longer essential for survival, collectively termed androgen pathway independent prostate cancer (APIPC) (Nelson, 2012). A subset of these cancers express markers of neuroendocrine differentiation, and transdifferentiation to a squamous phenotype has also been described in resistance to hormonal therapy (Humphrey, 2012); however, the molecular mechanisms underlying transition to APIPC are not fully characterized. Specifically, we hypothesize that APIPC represents a diversity of phenotypes and dependencies; a comprehensive understanding of these mechanisms would identify potential therapeutic targets for intervention, and would also allow for biomarker discovery to stratify patients for likelihood of response to targeted therapies (Choudhury, Eeles, *et al*., 2012). Thus, the signaling pathways described here warrant further study in this patient population.

REFERENCES

Abrahamsson PA. Neuroendocrine differentiation in prostatic carcinoma. Prostate. 1999 May;39(2):135-48.

Araujo JC, Trudel GC, Saad F, *et al*. Docetaxel and dasatinib or placebo in men with metastatic castration-resistant prostate cancer (READY): a randomised, double-blind phase 3 trial. Lancet Oncol. 2013 Dec;14(13):1307-16.

Attard G, Reid AH, A'Hern R, Parker C, Oommen NB, Folkerd E, Messiou C, Molife LR, Maier G, Thompson E, Olmos D, Sinha R, Lee G, Dowsett M, *et al.* (2009) Selective inhibition of CYP17 with abiraterone acetate is highly active in the treatment of castration-resistant prostate cancer. J Clin Oncol. 2009 Aug 10;27(23):3742-8. http://jco.ascopubs.org/content/27/23/3742.long

Belham C, Comb MJ, Avruch J. Identification of the NIMA family kinases NEK6/7 as regulators of the p70 ribosomal S6 kinase. Curr Biol. 2001 Aug 7;11(15):1155-67.

Belham C, Roig J, Caldwell JA, *et al*. A mitotic cascade of NIMA family kinases. Nercc1/Nek9 activates the Nek6 and Nek7 kinases. J Biol Chem. 2003 Sep 12;278(37):34897-909.

Berger, R., Febbo, P.G., Majumder, P.K., Zhao, J.J., Mukherjee, S., Signoretti, S., *et al.* (2004). Androgen-induced differentiation and tumorigenicity of human prostate epithelial cells. Cancer Res *64*, 8867-8875. http://cancerres.aacrjournals.org/content/64/24/8867.long

Bian Z, Liao H, Zhang Y, *et al*. Never in mitosis gene A related kinase-6 attenuates pressure overload-induced activation of the protein kinase B pathway and cardiac hypertrophy. PLoS One. 2014 Apr 24;9(4):e96095.

Bosco A, Ehteshami S, Stern DA, Martinez FD. Decreased activation of inflammatory networks during acute asthma exacerbations is associated with chronic airflow obstruction. Mucosal Immunol. 2010 Jul;3(4):399-409. doi: 10.1038/mi.2010.13. Epub 2010 Mar 24.

Cao X, Xia Y, Yang J, *et al*., Clinical and biological significance of never in mitosis gene A-related kinase 6 (NEK6) expression in hepatic cell cancer. Pathol Oncol Res. 2012 Apr;18(2):201-7.

Carver BS, Chapinski C, Wongvipat J, *et al*. Reciprocal feedback regulation of PI3K and androgen receptor signaling in PTEN-deficient prostate cancer. Cancer Cell. 2011 May 17;19(5):575-86.

Chen J, Li L, Zhang Y, *et al*. Interaction of Pin1 with Nek6 and characterization of their expression correlation in Chinese hepatocellular carcinoma patients. Biochem Biophys Res Commun. 2006 Mar 24;341(4):1059-65.

Cheon H, Holvey-Bates EG, Schoggins JW, *et al*. IFNβ-dependent increases in STAT1, STAT2, and IRF9 mediate resistance to viruses and DNA damage. EMBO J. 2013 Oct 16;32(20):2751-63.

Choudhury AD, Eeles R, Freedland SJ, *et al*. The role of genetic markers in the management of prostate cancer. Eur Urol. 2012 Oct;62(4):577-87.

Choudhury AD, Kantoff PW. New agents in metastatic prostate cancer. J Natl Compr Canc Netw. 2012 Nov 1;10(11):1403-9.

Cruciat CM. Casein kinase 1 and Wnt/β-catenin signaling. Curr Opin Cell Biol. 2014 Dec;31:46-55. doi: 10.1016/j.ceb.2014.08.003. Epub 2014 Sep 15.

Dirmeier U, Hoffmann R, Kilger E, *et al*. Latent membrane protein 1 of Epstein-Barr virus coordinately regulates proliferation with control of apoptosis. Oncogene. 2005 Mar 3;24(10):1711-7.

Edwards, J., and Bartlett, J.M. (2005a). The androgen receptor and signal-transduction pathways in hormone-refractory prostate cancer. Part 1: Modifications to the androgen receptor. BJU Int *95*, 1320-1326.

Edwards J, Bartlett JM. (2005b) The androgen receptor and signal-transduction pathways in hormone-refractory prostate cancer. Part 2: Androgen-receptor cofactors and bypass pathways. BJU Int. 2005 Jun;95(9):1327-35.

Drake JM, Graham NA, Stoyanova T, *et al*. Oncogene-specific activation of tyrosine kinase networks during prostate cancer progression. Proc Natl Acad Sci U S A. 2012 Jan 31;109(5):1643-8.

Drake JM, Graham NA, Lee JK, *et al.* Metastatic castration-resistant prostate cancer reveals intrapatient similarity and interpatient heterogeneity of therapeutic kinase targets. Proc Natl Acad Sci U S A. 2013 Dec 3;110(49):E4762-9.

Grasso CS, Wu YM, Robinson DR, *et al*. The mutational landscape of lethal castration-resistant prostate cancer. Nature. 2012 Jul 12;487(7406):239-43.

Guo Z, Dai B, Jiang T, Xu K, Xie Y, Kim O, Nesheiwat I, Kong X, Melamed J, Handratta VD, *et al.* (2006) Regulation of androgen receptor activity by tyrosine phosphorylation. Cancer Cell. 2006 Oct;10(4):309-19. http://www.sciencedirect.com/science/article/pii/S1535610806002777

Hieronymus H, Lamb J, Ross KN, *et al*. Gene expression signature-based chemical genomic prediction identifies a novel class of HSP90 pathway modulators. Cancer Cell. 2006 Oct;10(4):321-30.

Hu Y, Song W, Cirstea D, Lu D, Munshi NC, Anderson KC. CSNK1α1 mediates malignant plasma cell survival.Leukemia. 2015 Feb;29(2):474-82.

Huang S, Gulzar ZG, Salari K, Lapointe J, Brooks JD, Pollack JR. Recurrent deletion of CHD1 in prostate cancer with relevance to cell invasiveness. Oncogene. 2012 Sep 13;31(37):4164-70.

Humphrey PA. Histological variants of prostatic carcinoma and their significance. Histopathology. 2012 Jan;60(1):59-74.

Järås M, Miller PG, Chu LP, *et al*. Csnk1a1 inhibition has p53-dependent therapeutic efficacy in acute myeloid leukemia. J Exp Med. 2014 Apr 7;211(4):605-12.

Jee HJ, Kim AJ, Song N, *et al*. Nek6 overexpression antagonizes p53-induced senescence in human cancer cells. Cell Cycle. 2010 Dec 1;9(23):4703-10.

Jeon YJ, Lee KY, Cho YY, Pugliese A, Kim HG, Jeong CH, *et al.* (2010) Role of NEK6 in tumor promoter-induced transformation in JB6 C141 mouse skin epidermal cells. J Biol Chem. 2010 Sep 3;285(36):28126-33. http://www.jbc.org/content/285/36/28126.long

Lam JS, Yamashiro J, Shintaku IP, *et al*. (2005). "Prostate stem cell antigen is overexpressed in prostate cancer metastases.". Clin. Cancer Res. 11 (7): 2591–6.

Lin, H.K., Yeh, S., Kang, H.Y., and Chang, C. (2001). Akt suppresses androgen-induced apoptosis by phosphorylating and inhibiting androgen receptor. Proc Natl Acad Sci U S A *98*, 7200-7205. http://www.pnas.org/content/98/13/7200.long

Lizcano JM, Deak M, Morrice N, *et al*. Molecular basis for the substrate specificity of NIMA-related kinase-6 (NEK6). Evidence that NEK6 does not phosphorylate the hydrophobic motif of ribosomal S6 protein kinase and serum- and glucocorticoid-induced protein kinase *in vivo*. J Biol Chem. 2002 Aug 2;277(31):27839-49.

Matsuda A, Suzuki Y, Honda G, *et al*. Large-scale identification and characterization of human genes that activate NF-kappaB and MAPK signaling pathways. Oncogene. 2003 May 22;22(21):3307-18.

Mendiratta P, *et al*. Genomic strategy for targeting therapy in castration-resistant prostate cancer. *J Clin Oncol.* 2009 Apr 20;27(12):2022-9.

Mulholland DJ, Tran LM, Li Y, *et al*. Cell autonomous role of PTEN in regulating castration-resistant prostate cancer growth. Cancer Cell. 2011 Jun 14;19(6):792-804.

Nassirpour R, Shao L, Flanagan P, *et al*. Nek6 mediates human cancer cell transformation and is a potential cancer therapeutic target. Mol Cancer Res. 2010 May;8(5):717-28.

Nelson PS. Molecular states underlying androgen receptor activation: a framework for therapeutics targeting androgen signaling in prostate cancer. J Clin Oncol. 2012 Feb 20;30(6):644-6.

O'Regan L, Fry AM. The Nek6 and Nek7 protein kinases are required for robust mitotic spindle formation and cytokinesis. Mol Cell Biol. 2009 Jul;29(14):3975-90.

Palanisamy N, Ateeq B, Kalyana-Sundaram S, Pflueger D, Ramnarayanan K, *et al.* (2010) Rearrangements of the RAF kinase pathway in prostate cancer, gastric cancer and melanoma. Nat Med. 2010 Jul;16(7):793-8. http://www.nature.com/nm/journal/v16/n7/full/nm.2166.html

Pienta, K.J., and Bradley, D. (2006). Mechanisms underlying the development of androgen-independent prostate cancer. Clin Cancer Res *12*, 1665-1671. http://clincancerres.aacrjournals.org/content/12/6/1665.long

Qin J, Lee HJ, Wu SP, Lin SC, Lanz RB, Creighton CJ, DeMayo FJ, Tsai SY, Tsai MJ. Androgen deprivation-induced NCoA2 promotes metastatic and castration-resistant prostate cancer. J Clin Invest. 2014 Nov;124(11):5013-26.

Ren K, Gou X, Xiao M, *et al*. The over-expression of Pim-2 promote the tumorigenesis of prostatic carcinoma through phosphorylating eIF4B. Prostate. 2013 Sep;73(13):1462-9.

Richards MW, O'Regan L, Mas-Droux C, *et al*. An autoinhibitory tyrosine motif in the cell-cycle-regulated Nek7 kinase is released through binding of Nek9. Mol Cell. 2009 Nov 25;36(4):560-70.

Scher HI, Fizazi K, Saad F, Taplin ME, *et al*; AFFIRM Investigators. Increased survival with enzalutamide in prostate cancer after chemotherapy. N Engl J Med. 2012 Sep 27;367(13):1187-97.

Schneider RK, Ademà V, Heckl D, *et al*. Role of casein kinase 1A1 in the biology and targeted therapy of del(5q) MDS. Cancer Cell. 2014 Oct 13;26(4):509-20.

Sequist LV, Waltman BA, Dias-Santagata D, *et al*. Genotypic and histological evolution of lung cancers acquiring resistance to EGFR inhibitors. Sci Transl Med. 2011 Mar 23;3(75):75ra26.

Sharifi N. Mechanisms of androgen receptor activation in castration-resistant prostate cancer. Endocrinology. 2013 Nov;154(11):4010-7.

Sharma NL, Massie CE, Ramos-Montoya A, *et al.* The androgen receptor induces a distinct transcriptional program in castration-resistant prostate cancer in man. Cancer Cell. 2013 Jan 14;23(1):35-47.

Smith MR, Sweeney CJ, Corn PG, *et al*. Cabozantinib in chemotherapy-pretreated metastatic castration-resistant prostate cancer: results of a phase II nonrandomized expansion study. J Clin Oncol. 2014 Oct 20;32(30):3391-9.

Stoyanova T, Cooper AR, Drake JM, *et al*. Prostate cancer originating in basal cells progresses to adenocarcinoma propagated by luminal-like cells. Proc Natl Acad Sci U S A. 2013 Dec 10;110(50):20111-6.

Subramanian A, Tamayo P, *et al.* (2005) Gene set enrichment analysis: a knowledge-based approach for interpreting genome-wide expression profiles. Proc Natl Acad Sci U S A. 2005 Oct 25;102(43):15545-50. http://www.pnas.org/content/102/43/15545.long

Sun, H., Fang, H., Chen, T., Perkings, R., and Tong, W., "GOFFA: Gene Ontology For Functional Analysis - Software for gene ontology-based functional analysis of genomic and proteomic data." BMC Bioinformatics, 7(Suppl 2):S23, 2006.

Takeno A, Takemasa I, Doki Y, *et al*. Integrative approach for differentially overexpressed genes in gastric cancer by combining large-scale gene expression profiling and network analysis. Br J Cancer. 2008 Oct 21;99(8):1307-15.

Tao S, He H, Chen Q. ChIP-seq analysis of androgen receptor in LNCaP cell line. Mol Biol Rep. 2014 Sep;41(9):6291-6.

Taylor BS, Schultz N, Hieronymus H, Gopalan A, Xiao Y, Carver BS, Arora VK, Kaushik P, Cerami E, Reva B, *et al.* (2010) Integrative genomic profiling of human prostate cancer. Cancer Cell. 2010 Jul 13;18(1):11-22. http://www.sciencedirect.com/science/article/pii/S1535610810002382

Tran CP, Lin C, Yamashiro J, Reiter RE (2003). Prostate stem cell antigen is a marker of late intermediate prostate epithelial cells. Mol. Cancer Res. 1 (2): 113–21.

Tran, C., Ouk, S., Clegg, N.J., Chen, Y., Watson, P.A., Arora, V., Wongvipat, J., *et al.* (2009). Development of a second-generation antiandrogen for treatment of advanced prostate cancer. Science *324*, 787-790.http://www.sciencemag.org/content/324/5928/787.full

van Dorst EB, van Muijen GN, Litvinov SV, Fleuren GJ. The limited difference between keratin patterns of squamous cell carcinomas and adenocarcinomas is explicable by both cell lineage and state of differentiation of tumour cells. J Clin Pathol. 1998 Sep;51(9):679-84.

Vaz Meirelles G, Ferreira Lanza DC, da Silva JC, Santana Bernachi J, Paes Leme AF, Kobarg J. Characterization of hNek6 interactome reveals an important role for its short N-terminal domain and colocalization with proteins at the centrosome. J Proteome Res. 2010 Dec 3;9(12):6298-316.

Wallace TA, Prueitt RL, Yi M, *et al*. Tumor immunobiological differences in prostate cancer between African-American and European-American men. Cancer Res. 2008 Feb 1;68(3):927-36.

Wang Y, Lee YM, Baitsch L, *et al*. MELK is an oncogenic kinase essential for mitotic progression in basal-like breast cancer cells. Elife. 2014 May 20;3:e01763.

Weichselbaum RR, Ishwaran H, Yoon T, *et al*. An interferon-related gene signature for DNA damage resistance is a predictive marker for chemotherapy and radiation for breast cancer. Proc Natl Acad Sci U S A. 2008 Nov 25;105(47):18490-5.

Whang YE, Armstrong AJ, Rathmell WK, Godley PA, Kim WY, Pruthi RS, Wallen EM, Crane JM, Moore DT, Grigson G, Morris K, Watkins CP, George DJ. (2011) A phase II study of lapatinib, a dual EGFR and HER-2 tyrosine kinase inhibitor, in patients with castration-resistant prostate cancer. Urol Oncol. 2011 Mar 9.

Yeh, S., Lin, H.K., Kang, H.Y., Thin, T.H., Lin, M.F., and Chang, C. (1999). From HER2/Neu signal cascade to androgen receptor and its coactivators: a novel pathway by induction of androgen target genes through MAP kinase in prostate cancer cells. Proc Natl Acad Sci U S A *96*, 5458-5463. http://www.pnas.org/content/96/10/5458.long

Yin MJ, Shao L, Voehringer D, Smeal T, Jallal B. The serine/threonine kinase Nek6 is required for cell cycle progression through mitosis. J Biol Chem. 2003 Dec 26;278(52):52454-60.

Yokoyama NN, Shao S, Hoang BH, Mercola D, Zi X. Wnt signaling in castration-resistant prostate cancer: implications for therapy. Am J Clin Exp Urol. 2014 Apr 15;2(1):27-44.

Zhang B, Zhang H, Wang D, *et al*. Never in mitosis gene A-related kinase 6 promotes cell proliferation of hepatocellular carcinoma via cyclin B modulation. Oncol Lett. 2014 Sep;8(3):1163-1168.

Zuo J, Ma H, Cai H, Wu Y, Jiang W, Yu L. An inhibitory role of NEK6 in TGFβ/Smad signaling pathway. BMB Rep. 2014 Dec 18.

SUPPORTING DATA

Figure 1. NEK6 confers androgen-independent tumor formation in a xenograft model of androgen-dependent prostate cancer. A. Tumor formation at 60 days for parental LHSR-AR cells and cells expressing NEK6 in female and castrated mice. B. Tumor formation at 60 days for parental LHMK-AR cells and cells expressing NEK6 in female mice. C. Inducible expression of NEK6 *in vitro* at 48 hours after addition of doxycycline, and waterfall plot of change in tumor volume of parental LHSR-AR cells and cells with inducible NEK6 expression formed in male mice, 30 days after castration and removal of testosterone pellet.

Figure 2. A. NEK6-mediated androgen-independent tumors are primarily squamous in histology and AR negative. Sections of tumors derived from parental LHSR-AR cells expressing GFP in male mice, and cells expressing NEK6 in female and castrated mice were stained with AR antibody (brown). B. Sections of tumors derived from LHSR-AR cells overexpressing NEK6 in male mice with implanted testosterone pellet harvested prior to castration (Day 0) and at 4, 8, and 12 days after castration.

Figure 3. A. Immunohistochemical staining at 20x magnification for NEK6 in prostate cancer tissue microarrays. Low (left and middle) and high grade (right) cases are represented, each core showing tumor infiltrating in between benign glands with higher expression seen in the tumor. B. Flow diagram for assessment of clinical correlates of patients with high vs. low NEK6 expression in tumors.

Figure 4. NEK6 is overexpressed in several prostate cancer cell lines compared to immortalized (RWPE, LH) and transformed (LHSR-AR) prostate epithelial cells. A. Expression of NEK6 and AR in prostate cell lines with Hsp90 as loading control B. Expression of NEK6 in CL-1, PC-3, and DU145 cells with doxycycline inducible expression of 2 shRNAs targeting NEK6 or a control targeting lacZ in the presence or absence of doxycycline (CL-1 and PC-3) or with doxycycline in the presence or absence of growth factor stimulation (DU145). C. Proliferation curves of cells cultured in the presence of doxycycline with cells in 60 mm plates, split and replated every 2-3 days as indicated. Average of 3 replicates for each condition is shown.

Figure 5. A. NEK6 can phosphorylate NCOA5 and FOXJ2 *in vitro* at the sites discovered in the phosphoproteomic screen. 293T cells were transfected with expression constructs for wild-type and mutant (S-to-D) versions of NCOA5 or FOXJ2 with a C-terminal V5 tag and immunoprecipitated with anti-V5 antibody. Eluates from 1/5 of the beads were assayed by V5 immunoblot; the remaining 4/5 was subjected to on-bead *in vitro* kinase assay with recombinant active GST-NEK6 (Sigma). B+C. Kinase assay performed as in (A) but with wild-type or mutant forms of FOXJ2 or NCOA5 as indicated: + indicates a mutation is present at that residue, - indicates that the residue is wild-type (lane 1 of each blot represents the wild-type protein). 5% of the input assayed by V5 immunoblot is shown in the left panels; the kinase assay is shown in the right panels. FOXJ2 has 10 S/T residues in an "acceptable" NEK6 phosphorylation motif; the six previously reported in phosphosite.org for FOXJ2 or homologous to a previously detected phosphorylation site in FOXJ3 were tested in this assay. NCOA5 has 5 S/T residues in an "acceptable" NEK6 phosphorylation motif; however, mutating Ser201 to aspartic acid dramatically decreased exogenous NCOA5 expression, so the remaining four sites were tested in this assay.

Figure 6. A. 293T cells were transfected with expression constructs for the indicated kinases with a C-terminal V5 tag and immunoprecipitated with anti-V5 antibody. Eluates from 1/4 of the beads were assayed by V5 immunoblot; the remaining 3/4 was subjected to on-bead *in vitro* kinase assay with recombinant active GST-NEK6 (Sigma). B+C. Kinase assay performed as in (A) but with wild-type or mutant forms of CSNK1A1 or YES1 as indicated: + indicates a mutation is present at that residue, - indicates that the residue is wild-type (lane 1 of each blot represents the wild-type protein). 5% of the input assayed by V5 immunoblot is shown in the left panels; the kinase assay is shown in the right panels.

Figure 7. A. Immunoblots of protein lysates of xenograft tumors derived from LHSR-AR cells transduced with doxycycline-inducible constructs for the expression of GFP or NEK6 in male mice, with doxycycline

maintained in the diet at time of harvest (+dox) or with doxycycline diet removed 7 days prior to harvest (-dox). Tumors were harvested from non-castrated mice (day 0) or 2 or 5 days after castration. Two exposures of the NEK6 immunoblot are shown. B. Venn diagrams (Venny REF) demonstrating overlap between upregulated genes (fold change>1.5, signal-to-noise>1) and downregulated genes (fold change<0.67, signal-to-noise<-1) with NEK6 wild-type vs. kinase-dead expression in LHSR-AR cells 6 hours after growth factor stimulation *in vitro* assayed by Affymetrix microarray (green) and with NEK6 overexpressing vs. control LHSR-AR xenograft tumors 2 days (blue) and 5 days (yellow) after castration assayed by RNASeq. Overlapping genes are indicated. C. Gene Set Enrichment Analysis performed on the gene expression signature mediated by NEK6 overexpression at day 5 after castration (GSEA pre-ranked based on ratio of classes to tumors without NEK6 overexpression). The top two curated gene sets (C2) from the molecular signatures database (MSigDB) correlated with the NEK6 signature are shown.

Figure 8. A. Gene Set Enrichment Analysis performed on the gene expression signature of control tumors at day 5 after castration (GSEA pre-ranked based on ratio of classes to tumors at day 2 after castration). The top gene set from MSigDB C2 correlated with genes decreased in expression after castration is genes involved in interferon alpha/beta signaling (http://www.reactome.org/cgi-bin/eventbrowser_st_id?ST_ID=REACT_25162); in addition two prostate cancer related gene sets are also highly correlated with this signature (ranked #'s 9 and 12): genes up-regulated in prostate tumors developed by transgenic mice overexpressing VAV3 (Liu *et al*., 2008) and genes up-regulated in prostate cancer samples from African-American patients compared to those from the European-American patients (Wallace *et al*., 2008). B. Genes downregulated in the control (-dox) tumors after castration (fold change <-1.5, signal-to-noise <-1 in the comparison of tumors harvested at day 5 and day 2) were plotted against the NEK6 signature at day 5 using GSEA pre-ranked (left) and compared with genes upregulated by NEK6 at day 5 (fold change >1.5, signal-to-noise >1 in the comparison of +dox to -dox tumors) by Venn diagram (right). The GO terms most highly enriched in this overlap are cytokine-mediated and type I interferon signaling pathways ($p=2x10^{-5}$). C. RNASeq was performed from 3 tumors inducibly expressing a phosphomimic form of CK1α (S96D+T129D+T287D) with continued doxycycline expression, and 3 matched tumors s/p doxycycline withdrawal 5 days after castration. Left: The correlation of genes upregulated by CK1α(D×3) with the NEK6 signature at day 5 by GSEA pre-ranked; middle: overlap of the upregulated genes; right: the correlation of the CK1α(D×3) signature with the Bosco Epithelial Differentiation Module (right).

Supplemental Figure 1. A. Immunoblots using Epitomics 3789-1 (left) and Santa Cruz H-50 (right) anti-NEK6 primary antibodies on protein lysates of LHSR-AR cells transduced with a doxycycline-inducible construct for the expression of NEK6 with (+) or without (-) the addition of doxycycline in the media for 48 hours. B. Immunohistochemistry of xenograft tumors derived from LHSR-AR cells transduced with doxycycline-inducible constructs for the expression of NEK6 in male mice, with doxycycline maintained in the diet at time of harvest (+doxycycline) or with doxycycline diet removed 7 days prior to harvest (-doxycycline). Tumors were harvested 5 days after castration. C. Percentage of NEK6 positive cells (defined as having cytoplasmic NEK6 staining intensity greater than two standard deviations above the median) plotted against mean cytoplasmic NEK6 staining intensity (normalized as a percentile rank in each TMA) of cells within histologically benign-appearing glandular tissue (left) and tumor tissue (right) from radical prostatectomy specimens of patients with prostate cancer. Each point represents composite data from all benign or tumor cores from an individual patient. The threshold for positivity was set as the discontinuity in the distribution of % positive cells (at 12%) as indicated by the dashed red lines.

Supplemental Figure 2. A. Luciferase activity detected in LNCaP cells transiently transfected with an AR reporter either alone (top) or in combination with an expression plasmid for NEK6 (bottom) incubated with concentrations of the synthetic androgen R1881 indicated. B. Doxycycline-inducible expression of NEK6 wild-type, kinase dead (K74M/K75M), AKT1 and RAF1 both untagged and with C-terminal V5 tag. Untagged versions were used for experiments described. C. Inducible expression of NEK6 does not increase expression of AR targets PSA or TMPRSS2 in LHSR-AR cells. Expression of TMPRSS2 and PSA were measured by

qPCR in the absence and presence of doxycycline to induce transgene expression and in the presence and absence of R1881 as indicated, with expression normalized to cells transduced with NEK6 K74M/K75M in the absence of doxycycline and R1881. D. NEK6 expression has neither a positive or negative effect on AR signaling as measured through published AR signatures. Gene expression changes conferred by inducible expression of wild-type NEK6 vs. kinase dead NEK6 six hours after growth factor stimulation were assayed in 3 biological replicates, and GSEA was used to assess enrichment of signatures positively correlated with AR activity in two data sets from the literature (Hieronymus *et al*., 2006; Mendiratta *et al*., 2009, Sharma *et al*., 2013).

Supplemental Figure 3. A. Immunohistochemistry of xenograft tumors derived from LHSR-AR cells transduced with doxycycline-inducible constructs for the expression of NEK6 in male mice, with doxycycline maintained in the diet at time of harvest (+doxycycline) or with doxycycline diet removed 7 days prior to harvest (-doxycycline). Tumors were harvested from non-castrated mice (day 0) or 2 or 5 days after castration. B. LHSR-AR cells expressing GFP or wild-type or mutant forms of NEK6 under a doxycycline inducible promoter, in the presence of doxycycline and absence of growth factor stimulation (lanes 1-4), with growth factor stimulation in the absence of doxycycline (lanes 5-9) and with growth factor stimulation in the presence of doxycycline (lanes 10-14). Immunoblots for phosphorylated forms of p70S6K at Thr412 and STAT3 at Ser727 demonstrate increases with growth factor stimulation (compare lanes 1-4 with lanes 10-14) but no increase in the presence of wild-type NEK6 (lanes 2, 12) as compared to kinase-dead NEK6 (lanes 1, 11).

Supplemental Figure 4. NEK6 overexpression does not lead to promotion of cell cycle progression or antagonism of the p53 pathway in LHSR-AR cells. A. Cell cycle profiles of cells with and without NEK6 overexpression. LHSR-AR cells transduced with doxycycline-inducible NEK6 were cultured in the presence (bottom profiles) or absence (top profiles) of doxycycline, starved from growth factors for 24 hours, and released into growth factor-containing media for the times indicated, then harvested and fixed for propidium iodide staining in comparison to asynchronously cycling cells B. Proliferation curves of LHSR-AR constitutively expressing lacZ or NEK6, average cell counts from 3 plates collected at the indicated time points plotted compared to previous time point with standard deviations. C. p53 pathway is inactive in LHSR-AR cells, and NEK6 expression does not rescue from cell death mediated by etoposide. LHSR-AR cells with constitutive expression (pLX304-) of lacZ vs. NEK6 or doxycycline-inducible expression (pTRIPz-) of NEK6 kinase dead (kd) vs. wild-type (wt) were exposed to etoposide at concentrations indicated vs. DMSO as vehicle control. Attached and floating cells were harvested and combined for immunoblotting.

Supplemental Figure 5. RNASeq was performed from 3 tumors inducibly expressing phosphomimic forms of **A.** FOXJ2 (S8D+T23D+S254D) **B.** YES1 (T295D+S524D) and **C.** NCOA5 (S21D+S96D+S151D) with continued doxycycline expression, and 3 matched tumors for each s/p doxycycline withdrawal 5 days after castration. The genes upregulated by FOXJ2(D×3) and YES1(D×2), but not NCOA5(D×3), were highly correlated with the NEK6 signature at day 5 by GSEA pre-ranked (left), with overlapping upregulated genes with NEK6 shown in the Venn diagrams (right). Blue represents differentiation process genes, red represents immune process genes, purple represents genes in both categories, and black represents genes in neither category.

Supplemental Figure 6. A+B. 293T cells were transfected with expression constructs for the indicated proteins with a C-terminal V5 tag and immunoprecipitated with anti-V5 antibody. Eluates from 1/4 of the beads were assayed by V5 immunoblot; the remaining 3/4 was subjected to on-bead *in vitro* kinase assay with recombinant active GST-NEK6 (Sigma).

Supplemental Table 1.

		AR Nuclear % score (0,1,2,3,4)[a]	AR Nuclear intensity[b]	AR % Cytoplasm score (0,1,2,3,4)[a]	AR Cytoplasm intensity[b]	notes
Male mice (positive control)	GFP 1 (one piece)	4	m **s**	3	w **m**	9.11.12
	GFP 1 (second piece)	3	w **m** s	1	w	
	GFP 2	4	m s	1	w	
	GFP3	4	s	4	m s	
Female mice	NEK6 1 (one piece)	2	m **s**	2	w m	
	NEK6 2 (few pieces)	1	w	1	w	
	NEK6 3	trace	most nuclei are neg; occasional nuclei show weak staining (<1-2%)	trace	most cytoplasm are neg; occasional cells show weak staining (<1-2%)	surface mouse skin is neg for AR
	AKT1	2	m **s**	3	w **m** s	
	CCL2	0 (very small sample)	0	0 (very small sample)	0	scant epithelial cells
	ERBB2	2	**w** m s	2	w m	
	KRASV12 1 (one piece)	0		0		
	KRASV12 2 (2 other pieces)	1	**m** s	2	w **m**	
	MEKDD	1	w	4	**w** m s	
	PIM1	<5%	w (rare strong, 3-4 cells)	2	m **s**	
	RAF1	1	w m	4	w **m**	two pieces show this staining pattern; third piece has weak cyto stain in <25%, and nuclear stain weak in <25%.
Castrated mice	NEK6 castr	most are neg; however, one tissue fragment shows up to 3+ Nuc score in ~25% of nuclei	0-3			

[a] AR % score: 0, 1(1-25%),2(25-50%), 3(50-75%), 4(75-100%)

[b] Intensity: w=Weak, m=Moderate, s=Strong (**bold** indicates predominant intensity)

Supplemental Table 2.

Gene Name	Site	q enriched (wt vs. kd)	q enriched (wt induced vs. uninduced)	modifiedsequence_localization
LIMCH1	S303	9.73E-64	1.72E-102	_SWSTATS(ph)PLGGERPFR_7
DROSHA	S357	7.81E-32	2.87E-68	_NTDSWAPPLEIVNHRS(ph)PS(ph)REK_18
FOXJ2	S8	4.12E-18	2.22E-06	_(ac)ASDLESS(ph)LTSIDWLPQLTLR_7
FOXO3	S7	1.06E-17	4.06E-54	_(ac)AEAPAS(ph)PAPLSPLEVELDPEFEPQSRPR_6
HUWE1	S2595	7.84E-13	1.09E-09	_LLGPSAAADILQLSSS(ph)LPLQSR_16
EPPK1	S1529	4.20E-12	2.03E-06	_QVS(ph)ARDLFR_3
COIL	S487	6.79E-12	1.13E-13	_KIDS(ph)PPIRR_4
SRGAP1	S932	6.79E-12	1.21E-25	_LLELTS(ph)SYSPDVSDYKEGR_7
SLC2A12	S244	6.95E-11	2.89E-05	_LRALS(ph)DTTEELTVIK_5
TRPS1	S843	2.12E-09	3.99E-13	_TLRDS(ph)PNVEAAHLARPIYGLAVETK_5
MTX1	S9	4.78E-06	3.80E-03	_(ac)MLLGGPPRS(ph)PR_9
OGFR	S349	9.83E-06	9.02E-07	_S(ph)VEPQDAGPLER_1
INTS3	S502	5.00E-05	2.61E-06	_FPEFCSSPS(ph)PPVEVK_9
TRA2B	S239	7.67E-05	3.27E-03	_S(ph)YRGGGGGGGGWR_1
LMO7	S926	9.02E-05	5.17E-02	_GISS(ph)LPR_4
SATB2	S20	9.20E-05	5.42E-02	_SGS(ph)PDVKGPPPVK_3
ATM	T1885	1.32E-04	1.83E-02	_STT(ph)PANLDSESEHFFR_3
PLEKHA6	S313	3.42E-04	2.86E-06	_KSS(ph)MNQLQQWVNLRR_3
LMO7	S895	3.62E-04	2.13E-01	_VSAS(ph)LPR_4
PAK6	S246	4.80E-04	8.11E-07	_HGSEEARPQSCLVGSATGRPGGEGS(ph)PS(ph)PK_25
HNRNPM	S633	6.05E-04	3.70E-04	_GNFGGS(ph)FAGSFGGAGGHAPGVAR_6
MLLT3	S302	2.20E-03	9.42E-02	_KKS(ph)SSEALFK_3
HNRNPA2B1	S324	2.41E-03	5.43E-03	_SGNFGGS(ph)RNMGGPYGGGNYGPGGSGGSGGYGGR_7
NCOA5	S96	2.52E-03	1.18E-01	_DLRDS(ph)RDFR_5
SETX	T2474	2.53E-03	1.92E-01	_SLT(ph)HPPTIAPEGSRPQGGLPSSKLDSGFAK_3
BCL6	S466	2.65E-03	2.40E-01	_SSSESHS(ph)PLYMHPPK_7
ATXN1	S811	2.94E-03	1.27E-03	_ICIEGRS(ph)NVGK_7
CDKN2AIP	S151	3.23E-03	1.47E-01	_VIEGKNS(ph)SAVEQDHAK_7
FAM21C	S288	3.49E-03	1.82E-01	_S(ph)RPTS(ph)FADELAAR_5
EPS8L1	T305	5.41E-03	3.80E-02	_AAGEGLLT(ph)LR_8
FOXA1	S307	5.42E-03	1.00E-01	_KDPSGASNPSADS(ph)PLHR_13
KLF4	T316	6.40E-03	6.99E-05	_TT(ph)PTLGLEEVLSSR_2
LMO7	S1593	6.56E-03	1.32E-02	_SHS(ph)PSASQSGSQLR_3
ZNF326	S131	8.20E-03	1.57E-01	_NQGGSS(ph)WEAPYSR_6
PLEKHG6	S645	2.05E-02	1.29E-02	_S(ph)APELPEGILK_1
RIPK3	S316	3.04E-02	1.70E-03	_RFS(ph)IPESGQGGTEMDGFRR_3
ZNF326	S106	3.98E-02	9.73E-09	_FGGS(ph)YGGRFESSYR_4
ERCC5	S156	4.94E-02	1.03E-01	_ENDLYVLPPLQEEEKHS(ph)S(ph)EEEDEKEWQER_17
ERCC5	S157	4.94E-02	1.03E-01	_ENDLYVLPPLQEEEKHS(ph)S(ph)EEEDEKEWQER_18
LIG1	S66	5.02E-02	9.97E-02	_VLGS(ph)EGEEEDEALS(ph)PAK_4
MYOF	S193	5.29E-02	9.46E-04	_RMLS(ph)NKPQDFQIR_4
ZDHHC18	S19	6.19E-02	1.13E-07	_(ac)MKDCEYQQISPGAAPLPAS(ph)PGAR_19
PBRM1	S353	6.53E-02	1.45E-09	_LSAITM(ox)ALQYGS(ph)ES(ph)EEDAALAAAR_12

EXPH5	S1444	7.11E-02	3.82E-02	_RSS(ph)WECTGSGR_3
SIPA1L3	S158	7.11E-02	5.33E-07	_SKDVEFQDGWPRS(ph)PGR_13
ATXN1	S238	7.85E-02	9.85E-02	_APGLITPGS(ph)PPPAQQNQYVHIS(ph)SSPQNTGR_9
KRT18	S323	8.16E-02	1.44E-01	_NLKASLENS(ph)LREVEAR_9
IRF2BP1	S453	9.61E-02	4.17E-02	_NVAEALGHSPKDPGGGGGPVRAGGAS(ph)PAASSTAQPPTQHR_26
DLG3	Y673	1.01E-01	1.62E-01	_RDNEVDGQDY(ph)HFVVSR_10
ATXN1	S775	1.02E-01	7.46E-03	_WS(ph)APESR_2
EXPH5	S341	1.12E-01	3.01E-02	_S(ph)LHFPATTQSK_1
RFX2	S28	1.27E-01	2.98E-02	_(ac)MQNSEGGADSPASVALRPSAAAPPVPAS(ph)PQR_28
PCYT1B	S315	1.59E-01	3.42E-02	_M(ox)LQALS(ph)PK_6
EPS8L1	T202	1.61E-01	2.35E-01	_AVIST(ph)VER_5
HIVEP2	S2300	1.81E-01	3.82E-02	_RGPHALQSSGPPSTPS(ph)SPR_17
ZNF608	S964	1.96E-01	4.92E-05	_SKASS(ph)PSDIISSKDSVVK_5
KLF3	S71	2.08E-01	2.39E-23	_S(ph)SPPSAGNSPSSLKFPSSHRR_2
ACLY	S481	2.24E-01	2.45E-04	_KAKPAMPQDSVPS(ph)PR_13
ZNF608	S1453	2.31E-01	4.83E-07	_DRHS(ph)PFGQR_4

Supplemental Table 3.

GeneNames	log2 sample:control median	totalIntensity	numSpectra	Unique peptides
NEK6	2.603	2.48E+12	118	16
ACTR2	2.419	2.44E+12	42	17
ACTR1A	2.426	2.41E+12	8	4
MYH9	2.651	1.49E+12	291	61
MYL6	2.724	1.28E+12	42	8
UBA52	1.995	2.46E+11	8	4
SFN	1.987	1.79E+11	22	8
FRAS1	4.813	1.53E+11	2	2
CORO1A	3.79	9.88E+10	3	2
GSN	2.555	7.40E+10	41	14
EEF1A1	2.025	6.04E+10	45	13
S100A8	1.85	5.65E+10	27	12
TUBB	2.159	4.58E+10	14	3
S100A9	1.325	4.51E+10	21	10
MYH10	2.501	3.80E+10	34	12
TUBB2C	2.115	3.18E+10	20	4
MYO6	2.184	3.05E+10	41	20
ARPC2	2.378	2.97E+10	40	17
MYH14	1.85	2.64E+10	16	7
UTP20	6.005	2.09E+10	4	2
ARPC4	2.567	2.05E+10	22	7
DBT	1.389	2.03E+10	21	9
FLNB	1.724	1.80E+10	53	29
TMOD1	3.374	1.74E+10	8	2
FLNA	2.156	1.70E+10	55	22
TMOD3	2.201	1.64E+10	27	11
IQGAP1	1.641	1.51E+10	27	15
EIF4A1	1.931	1.49E+10	21	10
MYO1E	2.371	1.41E+10	19	8
KIF5B	1.293	1.33E+10	7	6
HSPA8	1.543	1.32E+10	41	13
CNGB1	3.565	1.26E+10	3	2
CAPZB	1.846	1.07E+10	21	13
ACTN4	2.523	1.02E+10	14	7
MYL9	1.78	8.66E+09	12	4
PRDX4	2.438	7.98E+09	9	2
CDC37	2.483	7.74E+09	24	13
S100A4	3.195	7.18E+09	8	4
TUBB2A	1.997	7.12E+09	8	2
MYO18A	2.216	6.92E+09	19	17
SLC25A3	3.05	6.71E+09	10	5
S100A2	3.209	6.39E+09	11	6
MYO1D	2.363	6.20E+09	19	7
TPI1	1.311	5.70E+09	15	8
PSMD1	1.932	5.45E+09	3	3
ANXA2	1.802	5.22E+09	14	9
MYO1B	2.951	5.07E+09	10	5
ACTC1	2.188	5.03E+09	12	2
CALM1	2.67	4.93E+09	7	4
HSP90AA1	2.25	4.81E+09	14	10
TPM1	3.045	4.78E+09	6	5
NPM1	2.247	4.67E+09	6	5
ARPC5	1.533	4.55E+09	12	6
PRKDC	1.331	4.53E+09	16	12
SERPINB5	1.815	4.48E+09	17	11
EEF2	1.533	4.29E+09	20	15
TPM4	1.951	3.89E+09	7	5
PGAM5	1.324	3.84E+09	3	2
YWHAZ	2.909	3.55E+09	6	1
CRIP1	1.698	3.41E+09	5	3
RAN	1.751	3.30E+09	11	6
THOC3	2.879	3.23E+09	4	2
PLS3	1.543	3.19E+09	16	9
NEK9	2.06	2.91E+09	14	9
TPM4	2.075	2.87E+09	5	3
TUFM	1.592	2.82E+09	12	6
DSTN	2.356	2.68E+09	3	2
RUVBL2	1.737	2.65E+09	10	8
ANXA1	1.329	2.64E+09	15	7
SPRR1B	1.522	2.49E+09	9	6
YWHAG	2.889	2.48E+09	4	3

SPTBN2	2.007	2.48E+09	7	7
ALDOC	1.406	2.39E+09	3	2
DOCK7	2.047	2.32E+09	8	6
DNAJA2	1.743	2.23E+09	8	5
RUVBL1	2.108	2.17E+09	14	6
GNB1	2.124	2.02E+09	6	3
PCBP2	1.573	1.94E+09	6	3
CRIP2	2.268	1.91E+09	8	3
RAB7A	1.509	1.88E+09	14	6
SERPINB1	1.626	1.85E+09	6	4
TCP1	2.157	1.82E+09	11	8
ARPC1A	2.279	1.79E+09	6	6
LIMA1	2.646	1.77E+09	7	6
GNB2	2.532	1.73E+09	5	3
SLC2A1	3.03	1.72E+09	2	2
CLTA	2.27	1.70E+09	5	4
VCP	1.472	1.66E+09	12	6
HNRNPK	1.417	1.57E+09	5	4
SLC25A6	1.831	1.44E+09	9	3
RAB11B	1.291	1.40E+09	8	5
SEC61A1	2.093	1.39E+09	6	4
ZNF185	2.191	1.37E+09	5	5
PPIA	1.374	1.33E+09	17	10
NPEPPS	1.421	1.32E+09	12	10
AIF1L	2.351	1.30E+09	3	3
GNB2L1	1.616	1.29E+09	10	9
SETX	2.13	1.24E+09	4	2
PHGDH	1.6	1.24E+09	6	6
KIF21B	2.038	1.21E+09	4	3
AHNAK	1.377	1.21E+09	7	6
DNAJA4	2.71	1.20E+09	2	1
CCT3	1.365	1.20E+09	9	6
MAPK1	1.597	1.19E+09	3	3
PPP1CA	2.184	1.15E+09	4	4
AHCY	1.393	1.14E+09	7	4
PDCD6IP	1.369	1.12E+09	17	11
STT3A	2.571	1.11E+09	6	4
TEX15	2.183	1.10E+09	3	3
SQRDL	1.705	1.08E+09	4	3
CALML3	2.365	1.04E+09	7	4
NCL	1.393	1.04E+09	9	5
MYO5A	2.628	1.02E+09	5	3
SLC25A11	1.729	9.75E+08	7	3
HP1BP3	1.362	9.71E+08	7	6
TUBB6	1.576	9.46E+08	9	3
YME1L1	1.565	9.32E+08	2	2
CPNE3	1.498	8.91E+08	5	4
ATL3	1.423	8.90E+08	2	2
PHB	1.577	8.85E+08	5	3
DDOST	1.817	8.72E+08	4	3
CAMK2D	1.354	8.71E+08	9	6
SERPINB8	1.446	8.54E+08	3	3
HARS	2.995	8.41E+08	3	2
COPB2	2.197	7.95E+08	6	5
POTEKP	1.725	7.90E+08	3	1
TMED10	1.515	7.88E+08	3	3
S100A10	1.918	7.68E+08	2	1
KRAS	1.285	7.63E+08	3	2
NARS	1.771	7.54E+08	4	3
H2AFJ	1.726	7.44E+08	2	1
MYL12B	2.834	7.31E+08	2	1
CTTN	1.64	6.95E+08	7	7
KPNB1	1.733	6.91E+08	3	3
LAD1	1.318	6.69E+08	3	2
YWHAH	2.803	6.58E+08	4	3
HSPH1	2.016	6.27E+08	8	6
SERPINB13	1.343	5.93E+08	3	3
SSR4	1.925	5.92E+08	2	1
COPB1	2.574	5.86E+08	5	3
MYO5C	2.939	5.66E+08	3	3
PDLIM1	1.423	5.53E+08	4	4
PDLIM5	1.733	5.50E+08	4	2
PRDX6	2.199	5.49E+08	2	2

MCM5	1.941	5.49E+08	2	2
TPM1	3.063	5.31E+08	4	2
XPO1	1.629	5.31E+08	3	3
C22orf28	1.391	5.18E+08	5	5
SDR16C5	1.795	5.00E+08	6	3
PSMC6	1.433	4.99E+08	4	3
NEK7	1.287	4.97E+08	4	1
GSTP1	1.323	4.83E+08	6	3
ATP5O	1.373	4.81E+08	6	3
HSPA9	1.453	4.76E+08	6	4
CCT4	1.418	4.73E+08	5	2
HIST1H2BB	1.991	4.71E+08	2	1
CDK5RAP2	1.542	4.62E+08	2	2
ALDH1A1	1.93	4.50E+08	2	2
TUBA1C	1.418	4.41E+08	3	1
DHCR7	1.404	4.24E+08	3	2
EIF4A3	1.442	4.16E+08	3	2
NAP1L1	1.771	4.07E+08	3	1
GMFB	1.831	4.05E+08	4	3
CYFIP2	1.359	4.03E+08	5	5
PPP2R2A	1.373	4.01E+08	4	3
CDKAL1	2.115	3.99E+08	2	2
RAB5A	1.3	3.99E+08	4	2
ATP5C1	1.371	3.90E+08	4	3
CKB	1.775	3.89E+08	4	4
PSMC5	1.409	3.75E+08	3	3
CAPZA1	1.302	3.63E+08	3	2
SLC25A13	1.574	3.60E+08	3	1
NME2	1.266	3.60E+08	4	2
H2AFZ	1.392	3.49E+08	2	2
PSMC1	2.106	3.48E+08	4	3
HECTD1	1.35	3.46E+08	4	4
PPIB	1.443	3.44E+08	4	4
CTNND1	1.785	3.42E+08	2	2
SAMD9	2.206	3.40E+08	5	5
IKBKB	1.889	3.38E+08	2	2
ADH5	1.927	3.30E+08	2	2
UACA	1.533	3.29E+08	4	4
ATP1A1	1.685	3.17E+08	2	1
S100A11	1.47	3.13E+08	5	2
C5orf38	2.752	3.10E+08	2	2
ATAD3B	1.253	3.10E+08	2	2
CEP350	2.936	3.09E+08	2	2
RAB14	1.999	3.09E+08	3	3
RPS6KA3	2.241	3.06E+08	3	3
IARS	2.182	3.06E+08	2	2
DCTN1	1.341	2.96E+08	2	2
YES1	2.071	2.92E+08	3	3
TAGLN2	1.69	2.90E+08	3	3
MAP2K2	1.646	2.86E+08	2	2
DDB1	1.72	2.83E+08	3	3
XDH	1.432	2.78E+08	3	3
PCF11	1.932	2.74E+08	2	2
NAMPT	1.75	2.74E+08	3	3
CSNK1A1	2.1	2.55E+08	2	1
MT-CO2	1.385	2.52E+08	2	2
SVIL	2.039	2.51E+08	2	2
ESYT2	1.444	2.51E+08	3	3
PSMD14	1.693	2.50E+08	2	2
SFRS3	2.106	2.42E+08	2	1
YWHAE	2.248	2.38E+08	2	2
SEPT2	1.854	2.37E+08	3	2
RPS6KA1	2.005	2.25E+08	3	3
CORO1B	1.378	2.24E+08	4	2
RAB1B	1.89	2.17E+08	3	2
SNRPD3	1.277	2.15E+08	2	2
HSPA2	1.325	2.07E+08	2	2
VPS35	2.32	1.96E+08	2	2
VPS29	1.264	1.95E+08	2	2
AHCYL1	1.289	1.93E+08	2	2
DDX3X	2.104	1.91E+08	2	2
ACTR3	2.319	1.86E+08	2	2
TWF1	1.427	1.85E+08	3	2

FN1	1.328	1.85E+08	3	3
UNC45A	1.464	1.84E+08	3	3
HNRNPD	2.559	1.80E+08	3	2
DPYSL2	1.254	1.78E+08	4	3
CCT5	1.857	1.75E+08	3	2
TMX3	2.142	1.74E+08	3	3
CNN2	1.386	1.74E+08	2	2
RAB35	1.539	1.69E+08	2	2
CNP	1.57	1.59E+08	2	2
USO1	1.4	1.58E+08	2	2
GPI	1.409	1.52E+08	2	2
GNA13	1.75	1.50E+08	2	2
SULT2B1	1.347	1.46E+08	2	2
CSNK2B	2.274	1.40E+08	2	1
FARSA	1.727	1.36E+08	2	2
UBE2M	1.524	1.35E+08	2	2
CTPS	1.7	1.34E+08	3	2
CAD	1.952	1.25E+08	2	2
RCC2	1.918	1.23E+08	2	2
HAT1	1.832	1.18E+08	2	2
RRAS2	1.561	1.09E+08	3	1
ERGIC1	2.174	1.06E+08	2	2
ACSL3	1.33	1.03E+08	3	2
VAPA	1.68	9.73E+07	2	2
LARS	1.296	9.71E+07	4	4
TES	1.901	8.75E+07	2	2
ARPC5L	1.703	7.86E+07	2	2
TM9SF3	1.646	7.38E+07	2	2
TOLLIP	1.426	6.70E+07	2	2
FAM83H	1.339	6.26E+07	4	4
HK1	1.574	4.96E+07	2	2
TRIM29	1.68	4.61E+07	2	2
LY6D	1.673	4.31E+07	2	2
RHOC	1.526	3.97E+07	2	2
RAI14	2.015	2.95E+07	2	2
FAM49B	2.133	2.93E+07	3	3
CHMP4B	1.824	2.93E+07	2	2
LRCH1	1.735	1.34E+07	2	2
ILF2	1.744	9.68E+06	2	2
NAP1L4	1.916	9.44E+06	2	2
DPM1	1.756	3.86E+06	2	1

Supplemental Table 4

GO terms NEK6 wt vs. NEK6 kd +growth factor stimulation in vitro

GOID	GOTERM	Level	PVALUE	E Value	GeneHits
GO:0051240	positive regulation of multicellular organismal process	3	0.008297	3.42	6
GO:0008015	blood circulation	5	0.009059	3.92	5
GO:0003013	circulatory system process	4	0.009197	3.91	5
GO:0065008	regulation of biological quality	3	0.010748	1.73	19
GO:0048878	chemical homeostasis	5	0.012744	2.56	8
GO:0009968	negative regulation of signal transduction	4	0.016305	2.95	6
GO:0023057	negative regulation of signaling	3	0.022366	2.74	6
GO:0010648	negative regulation of cell communication	4	0.022577	2.74	6
GO:0010817	regulation of hormone levels	4	0.023326	3.08	5
GO:0051239	regulation of multicellular organismal process	3	0.023671	1.89	12

GO terms intersection of Castration Down (Day 2 to 5) and NEK6 s/p castration Day 5 Up

GOID	GOTERM	Level	PVALUE	E Value	GeneHits
GO:0045087	innate immune response	4	0.000041	7.31	7
GO:0052548	regulation of endopeptidase activity	7	0.000092	10.84	5
GO:0052547	regulation of peptidase activity	6	0.000108	10.48	5
GO:0051336	regulation of hydrolase activity	5	0.000419	5.01	7
GO:0006955	immune response	3	0.000871	3.87	8
GO:0006952	defense response	4	0.000988	3.79	8
GO:0009607	response to biotic stimulus	3	0.001305	4.87	6
GO:0006950	response to stress	3	0.002619	2.29	13
GO:0042221	response to chemical stimulus	3	0.003219	2.35	12
GO:0051707	response to other organism	3	0.003466	4.85	5

GO terms intersection of Castration Up (Day 2 to 5) and NEK6 s/p castration Day 5 Down

GOID	GOTERM	Level	PVALUE	E Value	GeneHits
GO:0009628	response to abiotic stimulus	3	0.001886	3.96	7
GO:0009653	anatomical structure morphogenesis	3	0.00525	2.19	13
GO:0043436	oxoacid metabolic process	5	0.005573	2.94	8
GO:0019752	carboxylic acid metabolic process	6	0.005573	2.94	8
GO:0006082	organic acid metabolic process	4	0.006347	2.87	8
GO:0042180	cellular ketone metabolic process	4	0.006541	2.86	8
GO:0010817	regulation of hormone levels	4	0.007475	4.09	5
GO:0048666	neuron development	5	0.008904	2.97	7
GO:0048812	neuron projection morphogenesis	7	0.009043	3.34	6
GO:0006508	proteolysis	5	0.014732	2.48	8

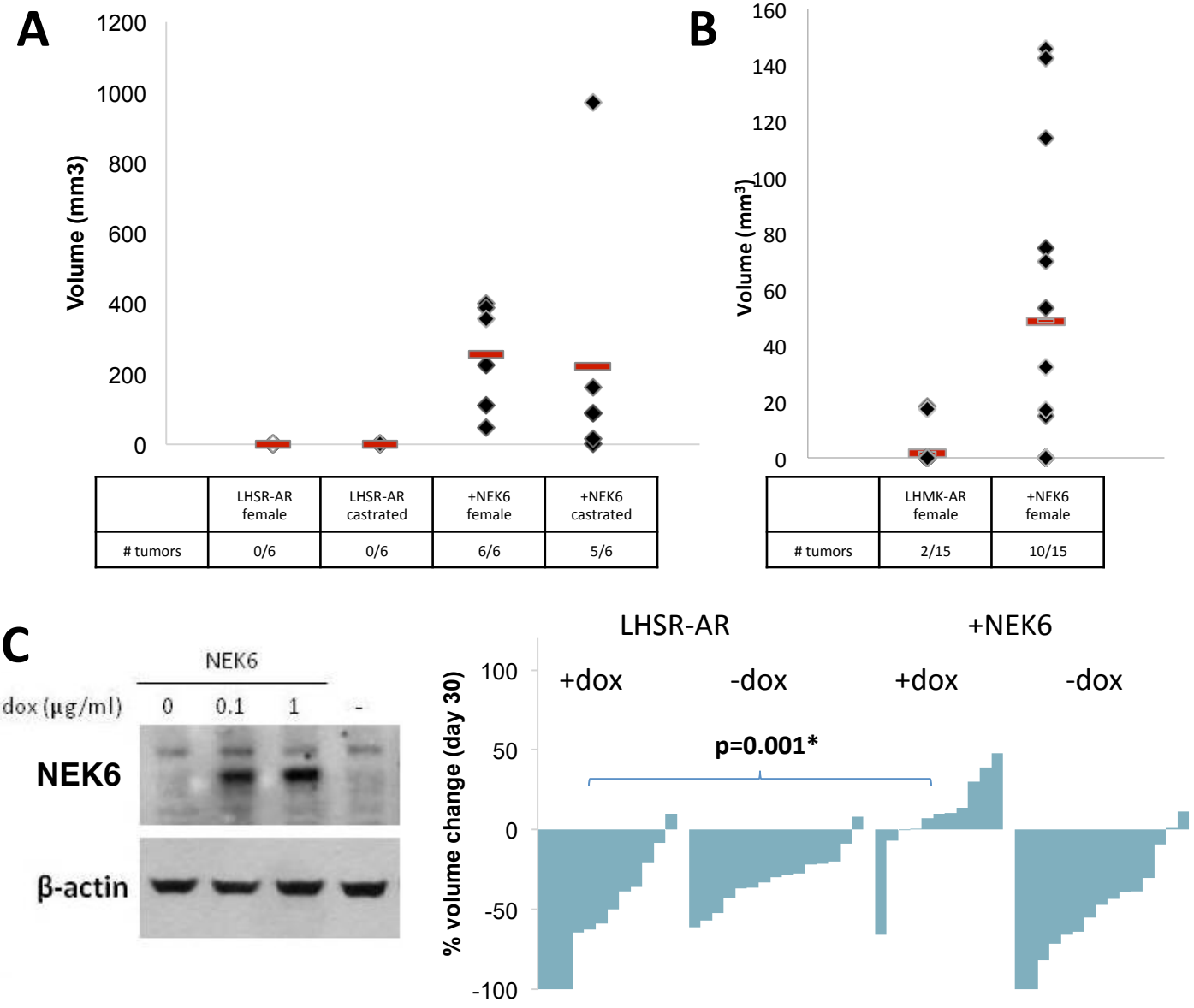
A
Volume (mm3)
1200
1000
800
600
400
200
0
LHSR-AR female
LHSR-AR castrated
+NEK6 female
+NEK6 castrated
tumors
0/6
0/6
6/6
5/6
B
Volume (mm³)
160
140
120
100
80
60
40
20
0
LHMK-AR female
+NEK6 female
tumors
2/15
10/15
C
NEK6
dox (µg/ml)
0
0.1
1
-
NEK6
β-actin
LHSR-AR
+NEK6
+dox
-dox
+dox
-dox
p=0.001*
% volume change (day 30)
100
50
0
-50
-100

Figure 1

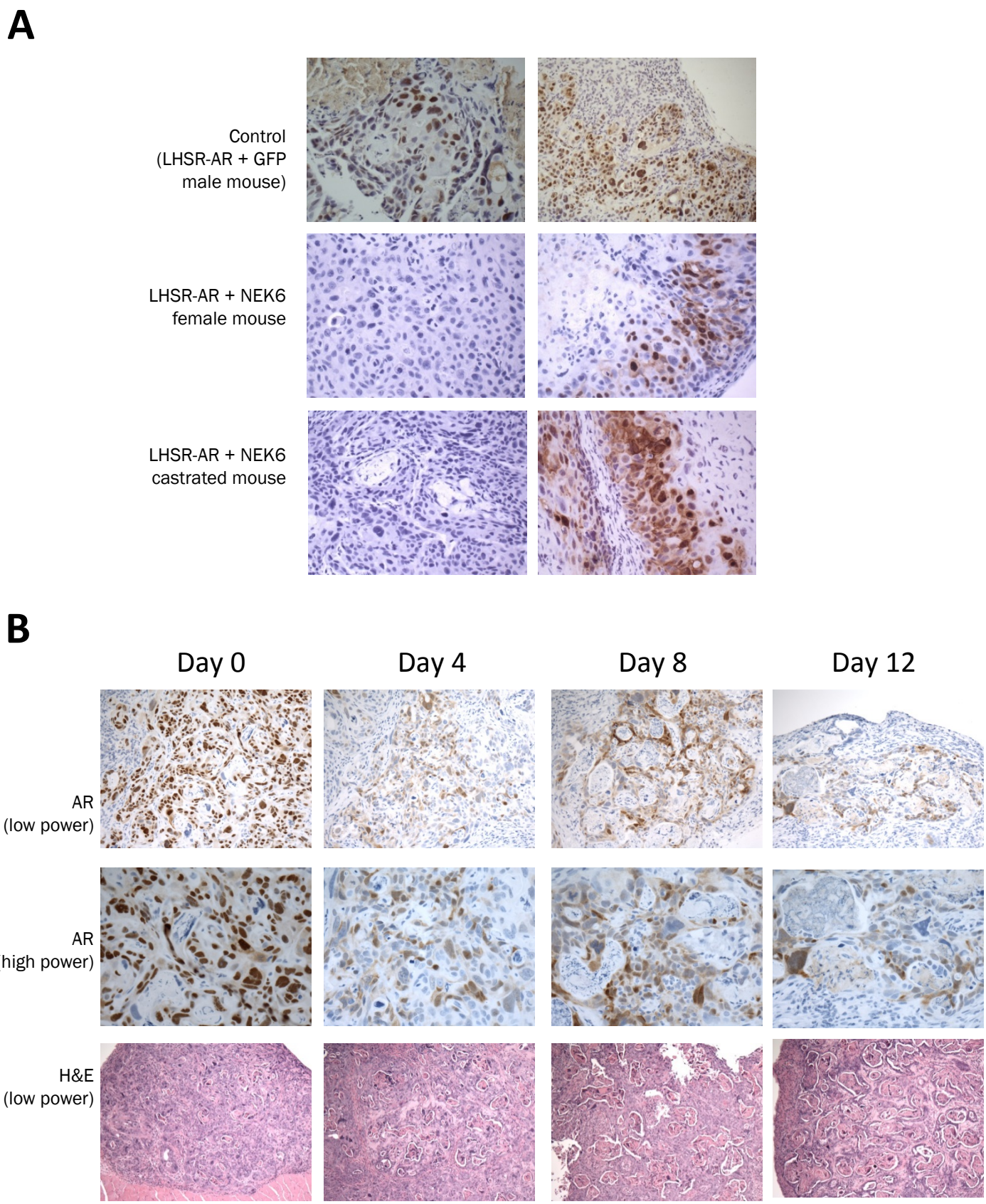
A
Control
(LHSR-AR + GFP
male mouse)
LHSR-AR + NEK6
female mouse
LHSR-AR + NEK6
castrated mouse
B
Day 0
Day 4
Day 8
Day 12
AR
(low power)
AR
(high power)
H&E
(low power)

Figure 2

A

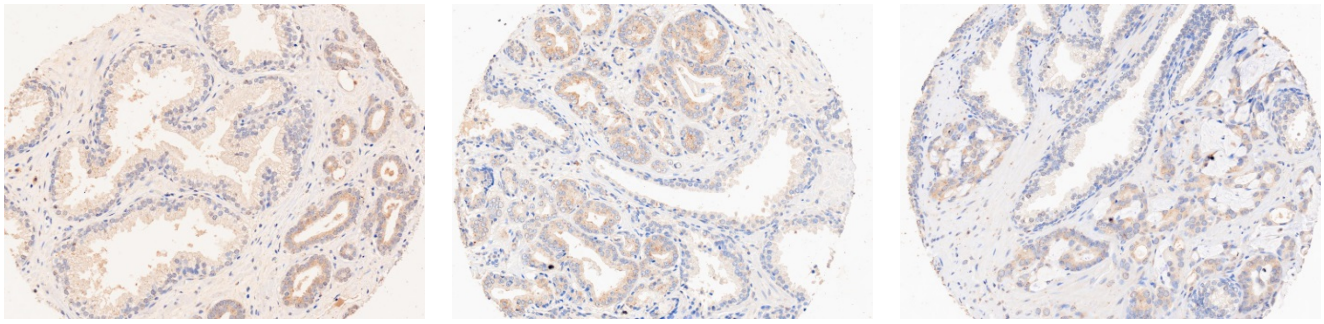

B

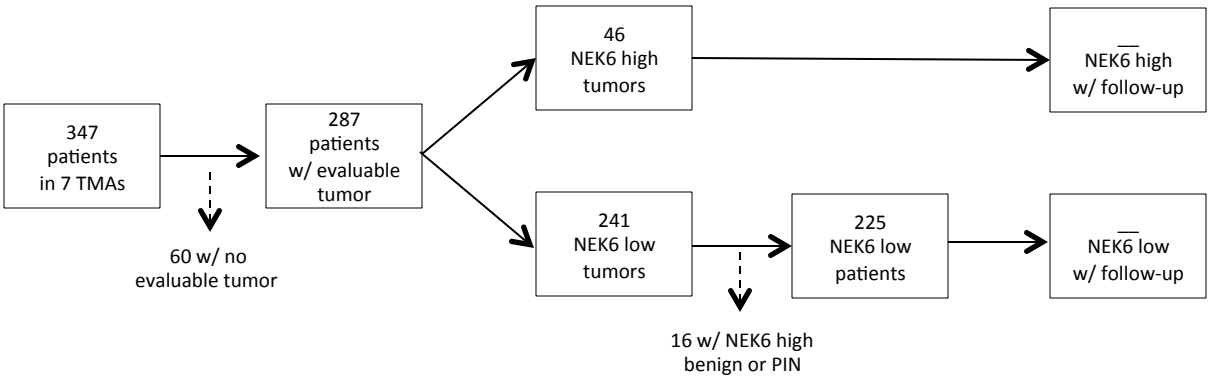
347 patients in 7 TMAs
60 w/ no evaluable tumor
287 patients w/ evaluable tumor
46 NEK6 high tumors
NEK6 high w/ follow-up
241 NEK6 low tumors
16 w/ NEK6 high benign or PIN
225 NEK6 low patients
NEK6 low w/ follow-up

Figure 3

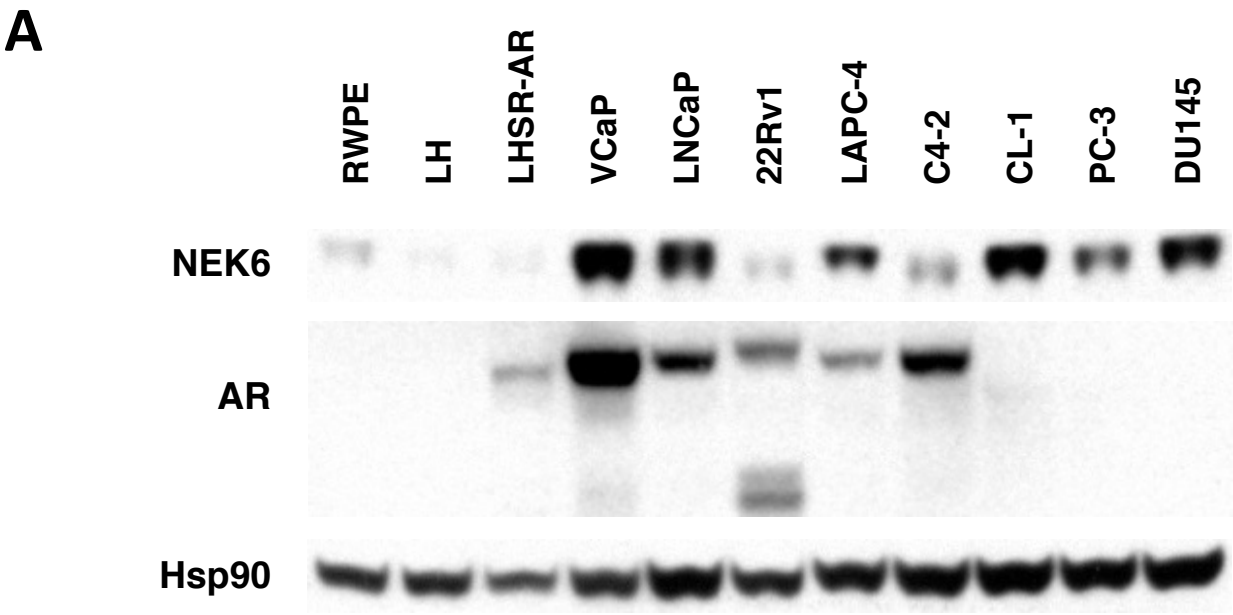
A
RWPE
LH
LHSR-AR
VCaP
LNCaP
22Rv1
LAPC-4
C4-2
CL-1
PC-3
DU145
NEK6
AR
Hsp90

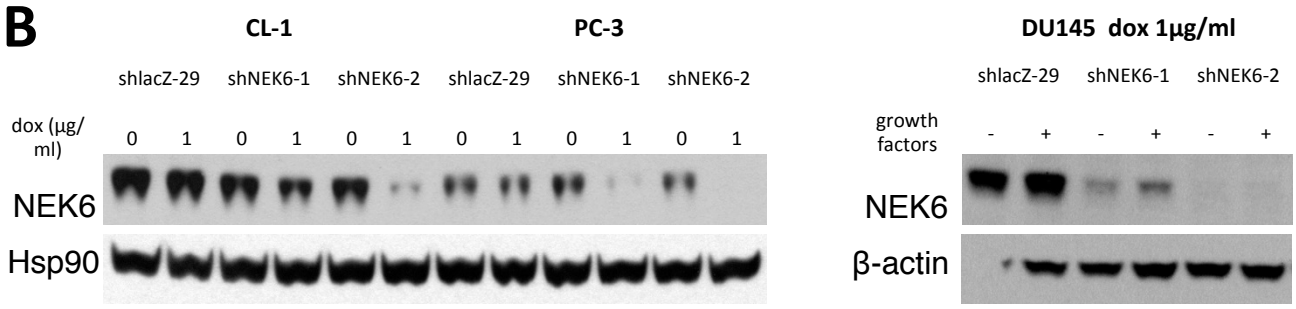
B
CL-1
PC-3
shlacZ-29
shNEK6-1
shNEK6-2
shlacZ-29
shNEK6-1
shNEK6-2
dox (µg/ml)
0 1 0 1 0 1 0 1 0 1 0 1
NEK6
Hsp90
DU145 dox 1µg/ml
shlacZ-29
shNEK6-1
shNEK6-2
growth factors
- + - + - +
NEK6
β-actin

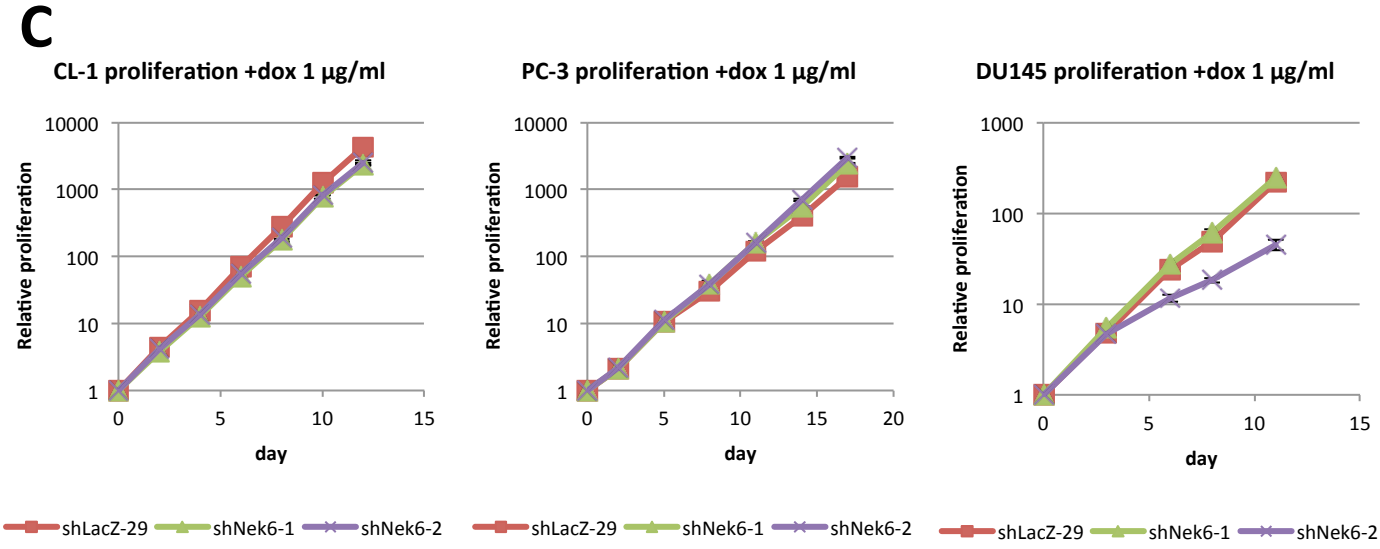
C
CL-1 proliferation +dox 1 µg/ml
PC-3 proliferation +dox 1 µg/ml
DU145 proliferation +dox 1 µg/ml
Relative proliferation
day
shLacZ-29
shNek6-1
shNek6-2

Figure 4

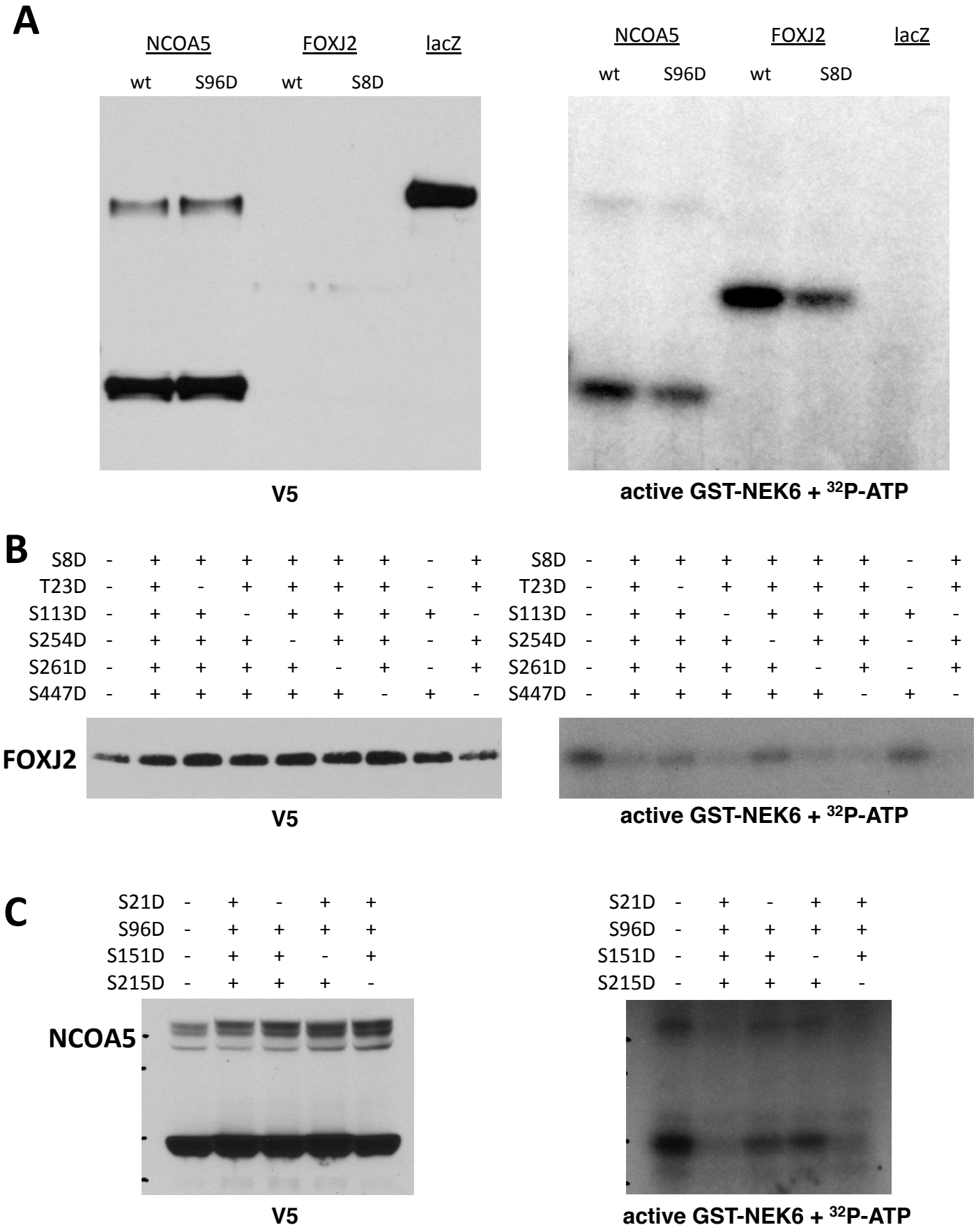
A
NCOA5
FOXJ2
lacZ
wt
S96D
wt
S8D
V5
NCOA5
FOXJ2
lacZ
wt
S96D
wt
S8D
active GST-NEK6 + 32P-ATP
B
S8D - + + + + + + - +
T23D - + - + + + + - +
S113D - + + - + + + + -
S254D - + + + - + + - +
S261D - + + + + - + - +
S447D - + + + + + - + -
FOXJ2
V5
S8D - + + + + + + - +
T23D - + - + + + + - +
S113D - + + - + + + + -
S254D - + + + - + + - +
S261D - + + + + - + - +
S447D - + + + + + - + -
active GST-NEK6 + 32P-ATP
C
S21D - + - + +
S96D - + + + +
S151D - + + - +
S215D - + + + -
NCOA5
V5
S21D - + - + +
S96D - + + + +
S151D - + + - +
S215D - + + + -
active GST-NEK6 + 32P-ATP

Figure 5

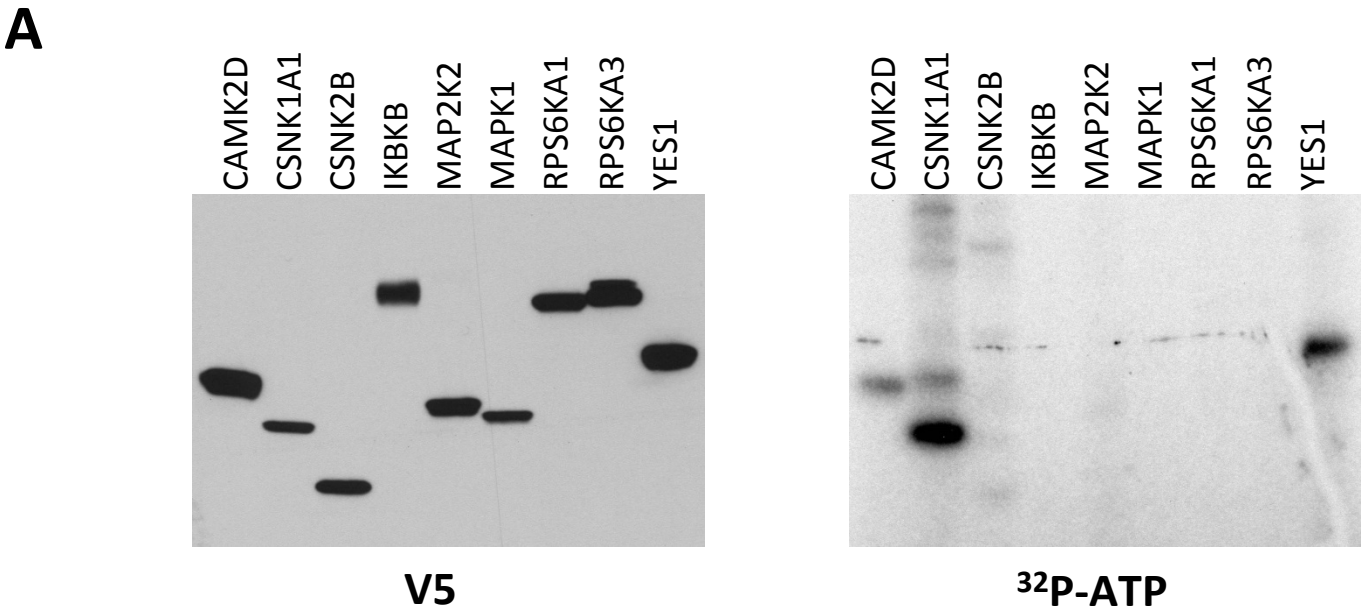
A
CAMK2D
CSNK1A1
CSNK2B
IKBKB
MAP2K2
MAPK1
RPS6KA1
RPS6KA3
YES1
V5
32P-ATP
B
S61D
S96D
T129D
T287D
T296D
CSNK1A1
V5
32P-ATP
C
S197D
T226D
T295D
S524D
YES1
V5
32P-ATP

Figure 6

A

pTRIPz-GFP						pTRIPz-NEK6																	
day 0			day 2			day 0						day 2						day 5					
+dox						-dox			+dox			-dox			+dox			-dox			+dox		
1	2	3	1	2	3	1	2	3	1	2	3	1	2	3	1	2	3	1	2	3	1	2	3

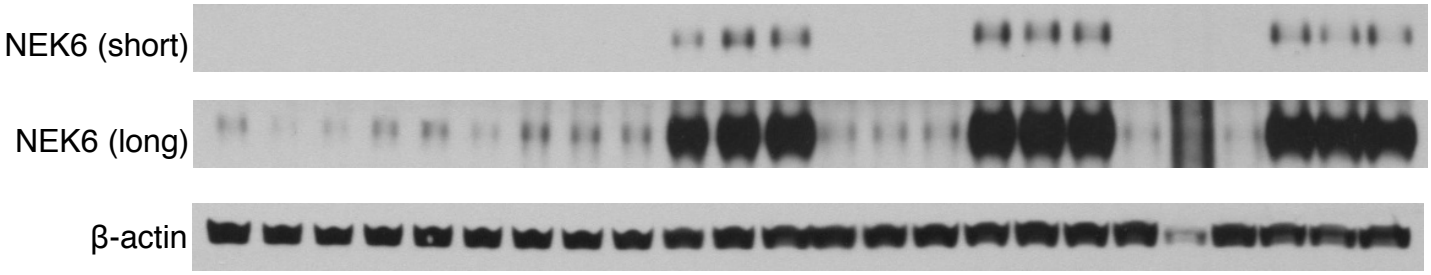

B

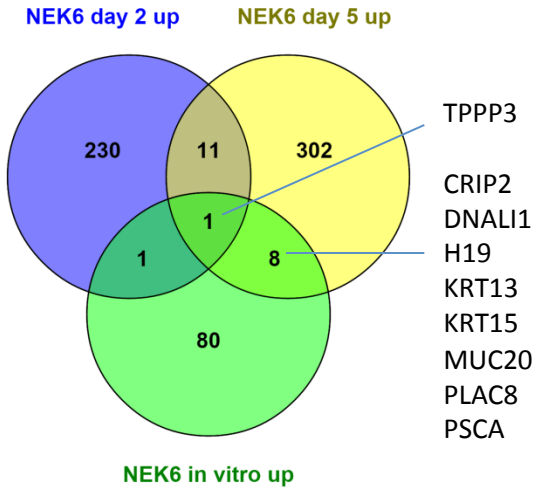

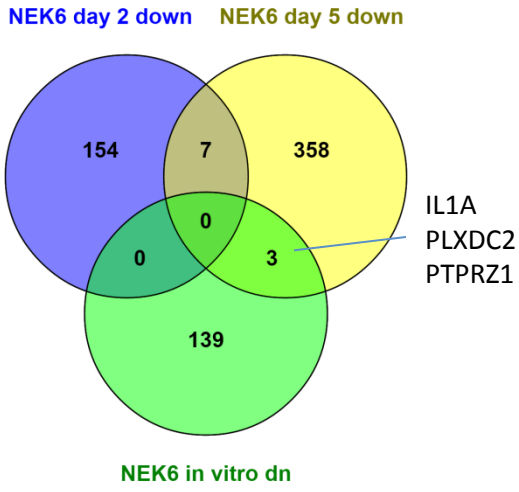

C

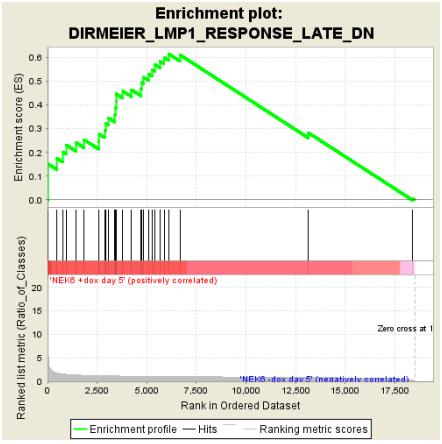

Enrichment Score (ES)	0.6142362
Normalized Enrichment Score (NES)	2.9263046
Nominal p-value	0.0
FDR q-value	7.961313E-4
FWER p-Value	0.001

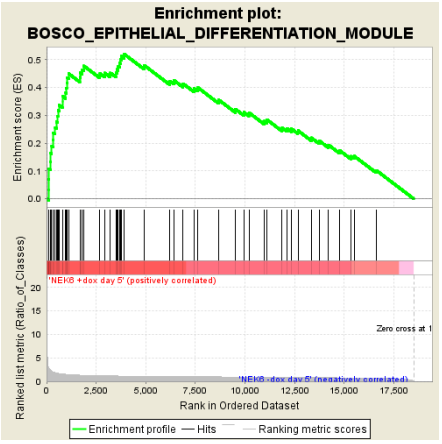

Enrichment Score (ES)	0.519851
Normalized Enrichment Score (NES)	2.9107523
Nominal p-value	0.0
FDR q-value	7.999157E-4
FWER p-Value	0.002

Figure 7

A

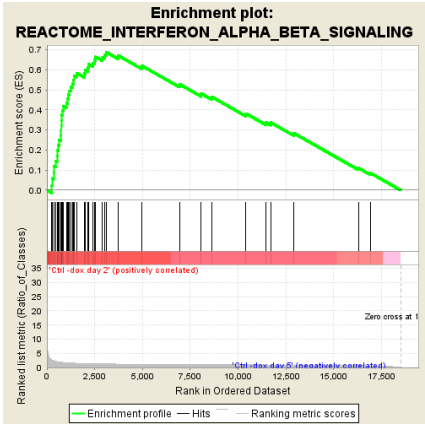

Enrichment Score (ES)	0.6873438
Normalized Enrichment Score (NES)	3.2027712
Nominal p-value	0.0
FDR q-value	0.0
FWER p-Value	0.0

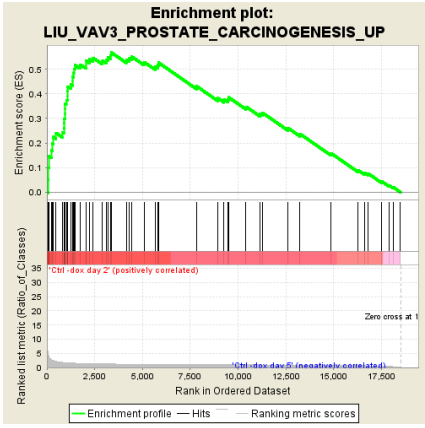

Enrichment Score (ES)	0.5693905
Normalized Enrichment Score (NES)	2.8814788
Nominal p-value	0.0
FDR q-value	0.0025325378
FWER p-Value	0.023

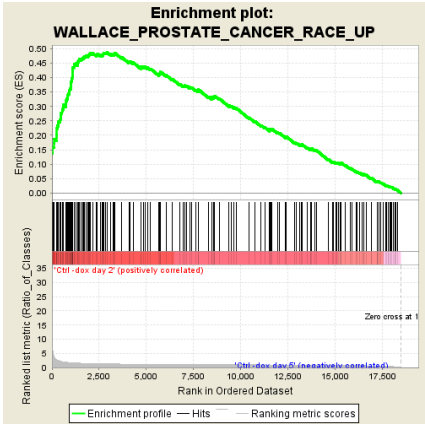

Enrichment Score (ES)	0.4878112
Normalized Enrichment Score (NES)	2.844538
Nominal p-value	0.0
FDR q-value	0.0030581069
FWER p-Value	0.037

B

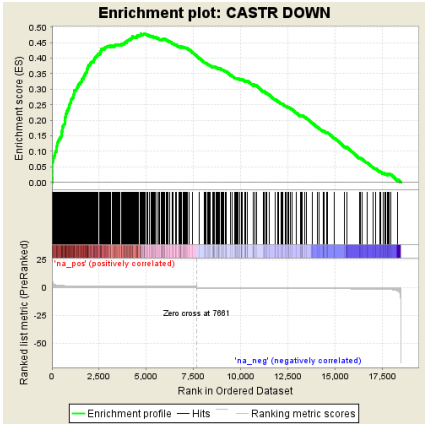

Enrichment Score (ES)	0.47908518
Normalized Enrichment Score (NES)	6.545397
Nominal p-value	0.0
FDR q-value	0.0
FWER p-Value	0.0

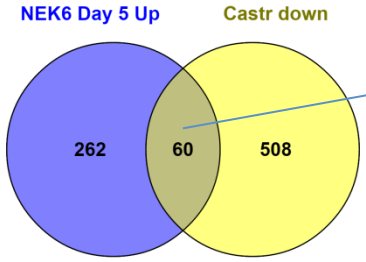

GO: developmental process	immune system process
DISP1	C4B
KRT8	CFB
KRT18	HSPH1
LY6E	IFI6
MAP1S	IRF7
PAX8	ISG15
PLAC8	ISG20
RHOC	PRG2
BST2	BST2
SH2B2	SH2B2
GO:	

C

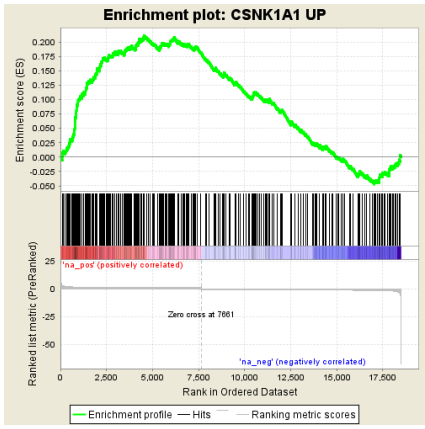

Enrichment Score (ES)	0.21139549
Normalized Enrichment Score (NES)	2.6029801
Nominal p-value	0.0
FDR q-value	0.0015906681
FWER p-Value	0.001

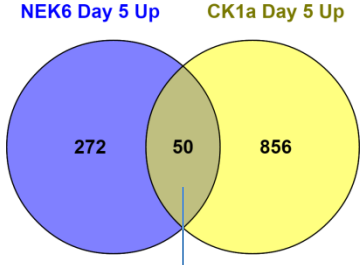

ATP6V1B1	PLA2G2A	CLU
CST3	PLAC8	RGCC
KRT4	RHCG	C4B
KRT8	RHOC	CTSD
KRT13	RHOU	LCN2
METRN	SPDEF	PHPT1
MSLN	SPRR3	
MUC1		

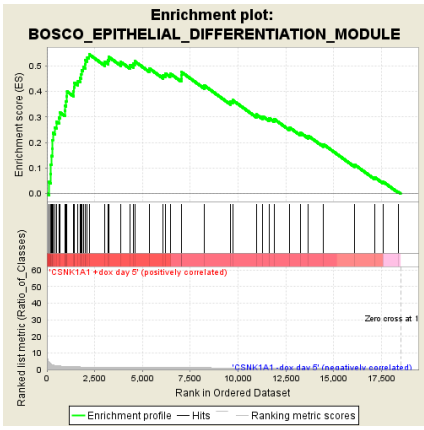

Enrichment Score (ES)	0.54472786
Normalized Enrichment Score (NES)	2.7282033
Nominal p-value	0.0
FDR q-value	0.68416107
FWER p-Value	0.948

Figure 8

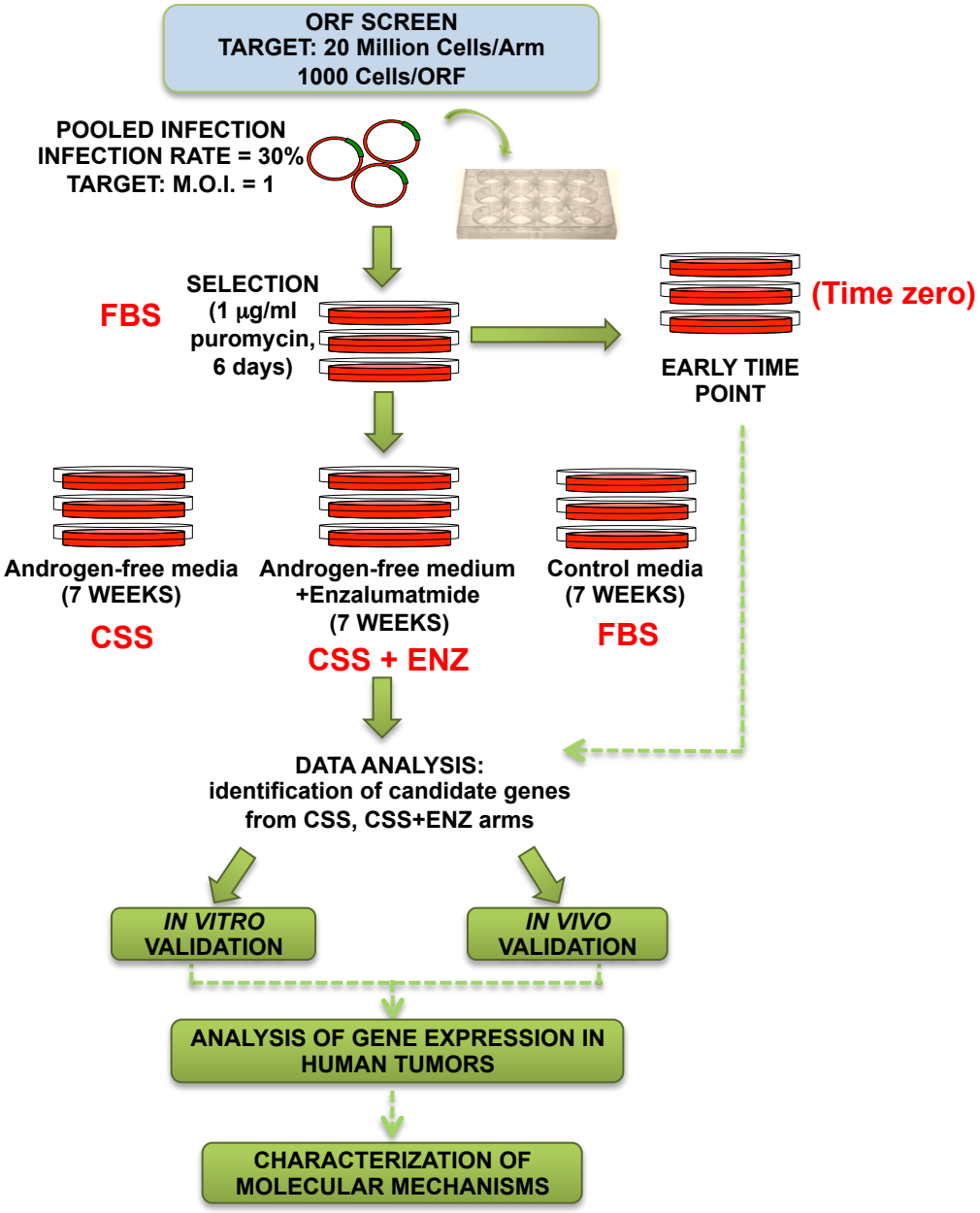
ORF SCREEN
TARGET: 20 Million Cells/Arm
1000 Cells/ORF
POOLED INFECTION
INFECTION RATE = 30%
TARGET: M.O.I. = 1
FBS
SELECTION
(1 µg/ml
puromycin,
6 days)
(Time zero)
EARLY TIME
POINT
Androgen-free media
(7 WEEKS)
CSS
Androgen-free medium
+Enzalumatmide
(7 WEEKS)
CSS + ENZ
Control media
(7 WEEKS)
FBS
DATA ANALYSIS:
identification of candidate genes
from CSS, CSS+ENZ arms
IN VITRO
VALIDATION
IN VIVO
VALIDATION
ANALYSIS OF GENE EXPRESSION IN
HUMAN TUMORS
CHARACTERIZATION OF
MOLECULAR MECHANISMS

Figure 9

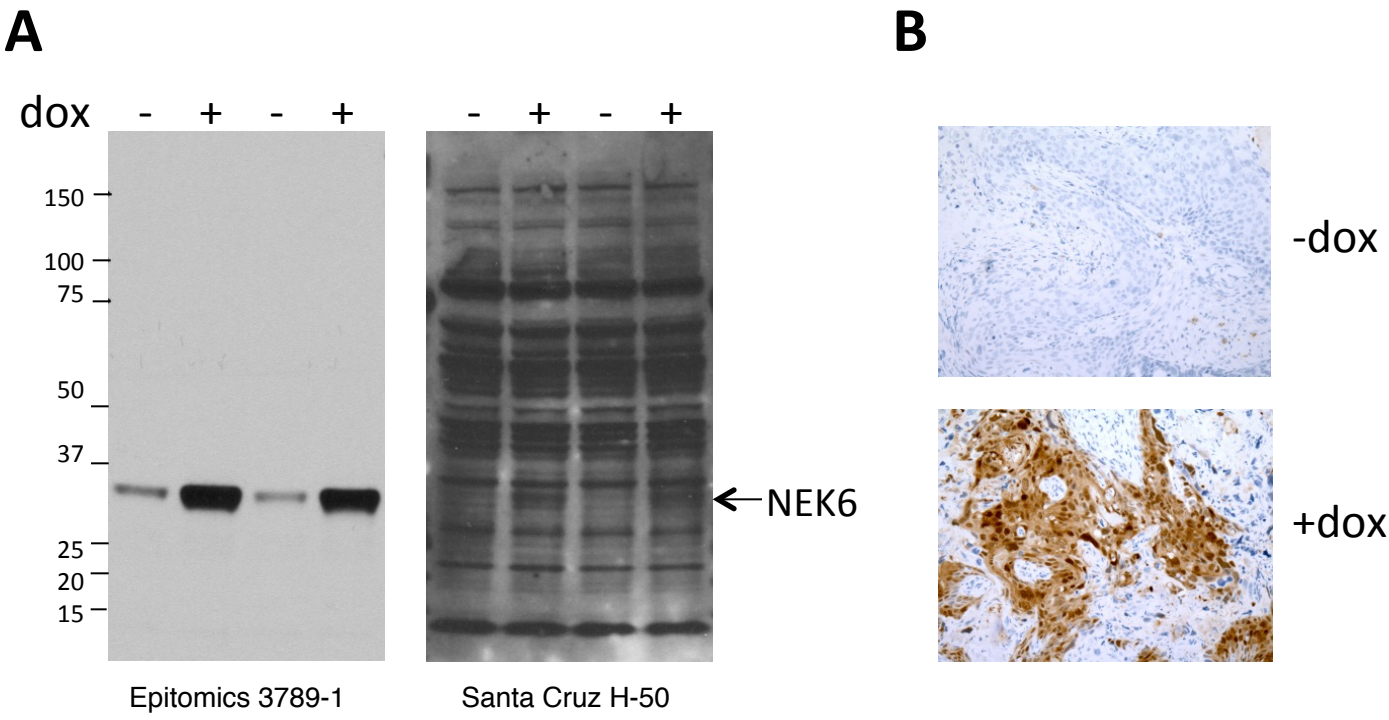

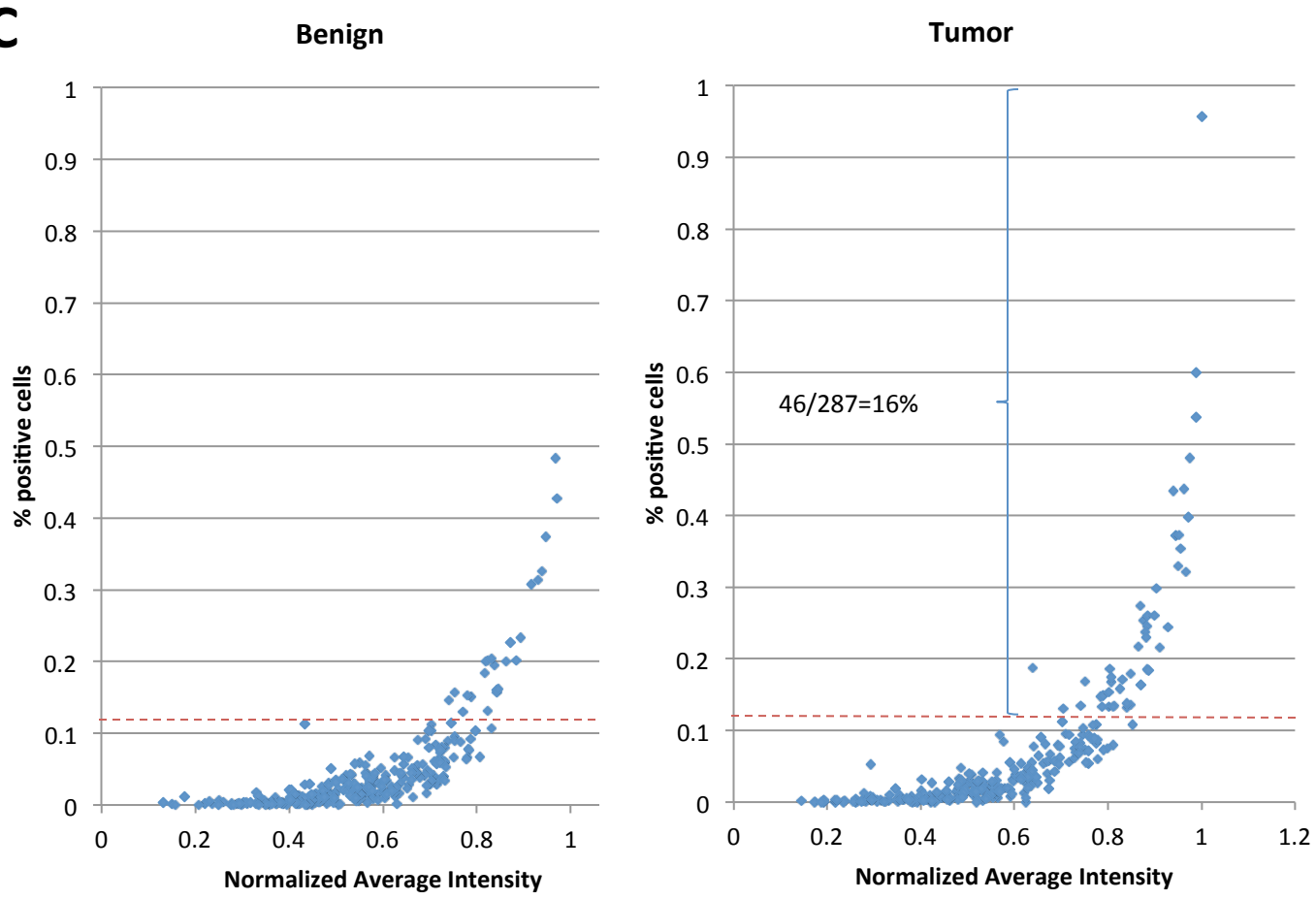

Supplemental Figure 1

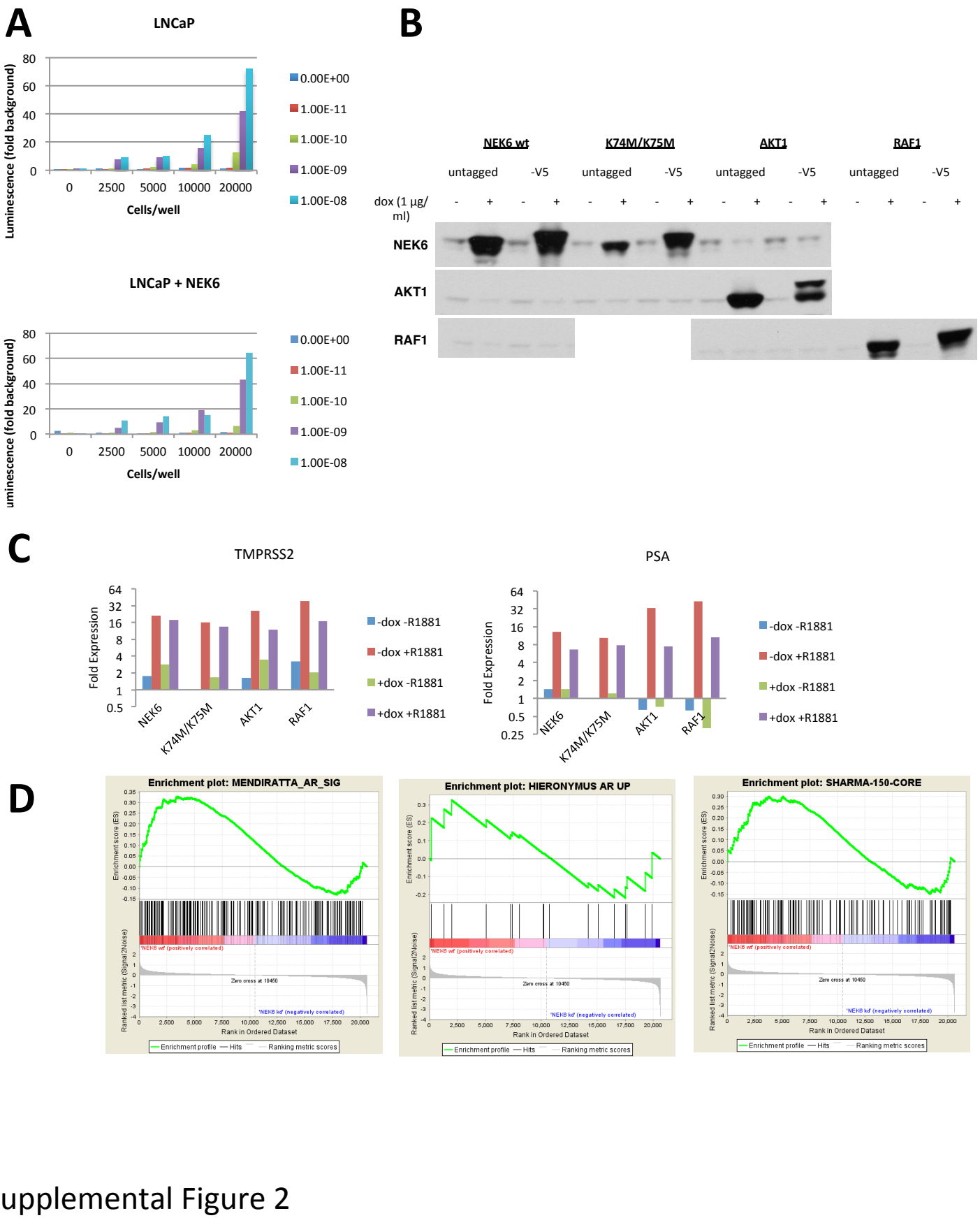

Supplemental Figure 2

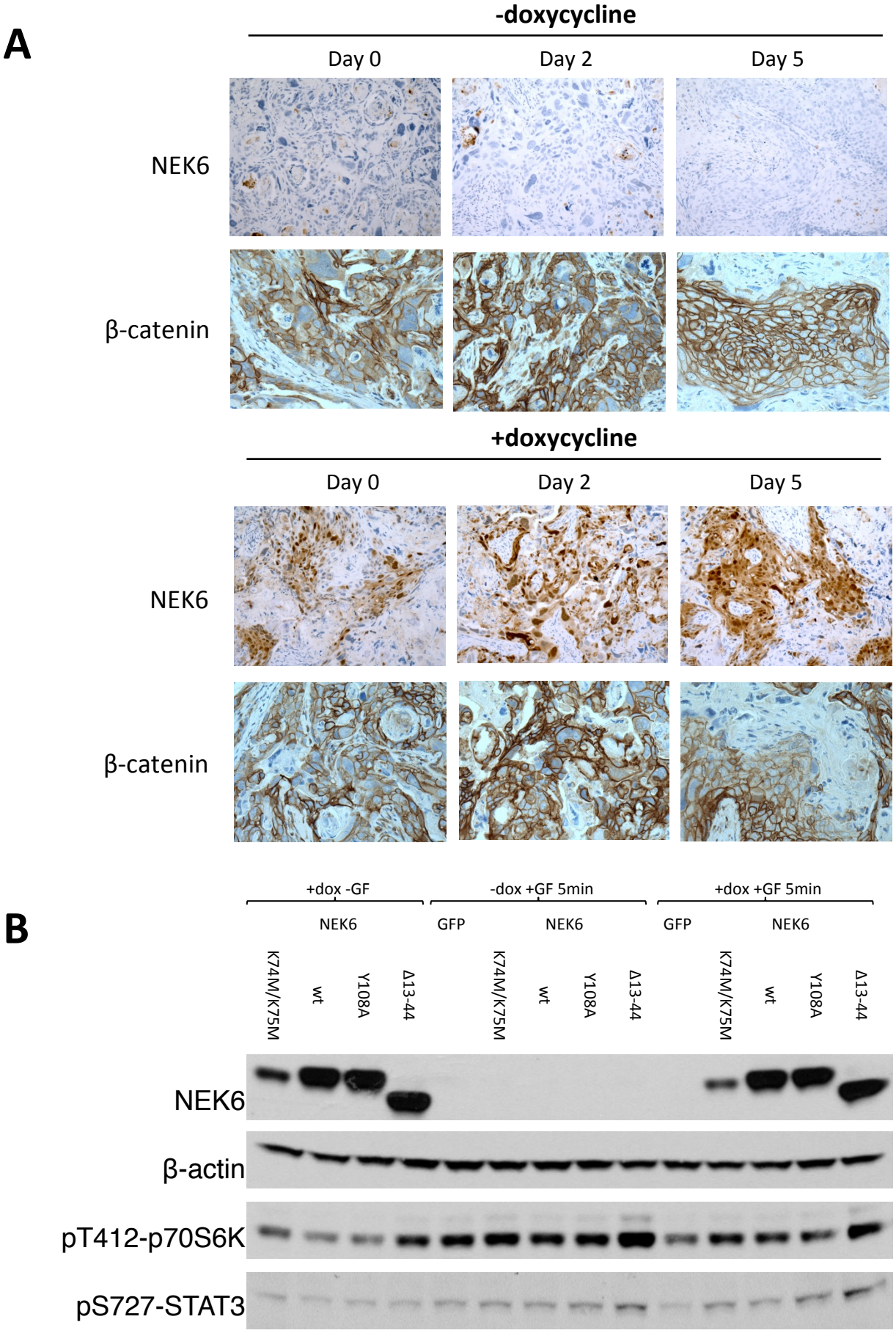

Supplemental Figure 3

A

-dox

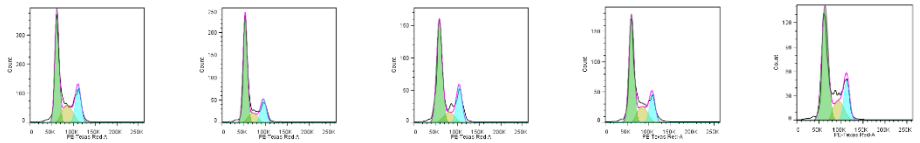

	async		0 h		4 h		8 h		24 h	
	-dox	+dox	-dox	+dox	-dox	+dox	-dox	+dox	-dox	+dox
G0/G1	54.5	54.2	69.2	67.8	58.9	57.1	57.6	51.6	51.6	50.9
S	15.5	16.2	8.4	7.1	13.6	13.1	16.9	16.9	19	17.8
G2/M	25	23.5	18.4	14.9	19.3	22.3	19.1	20	21.9	19.5
sub-G1	5.1	4.7	4.0	10.0	6.8	5.8	6.0	9.7	6.9	10

+dox

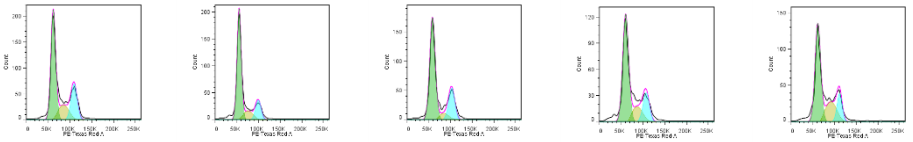

B

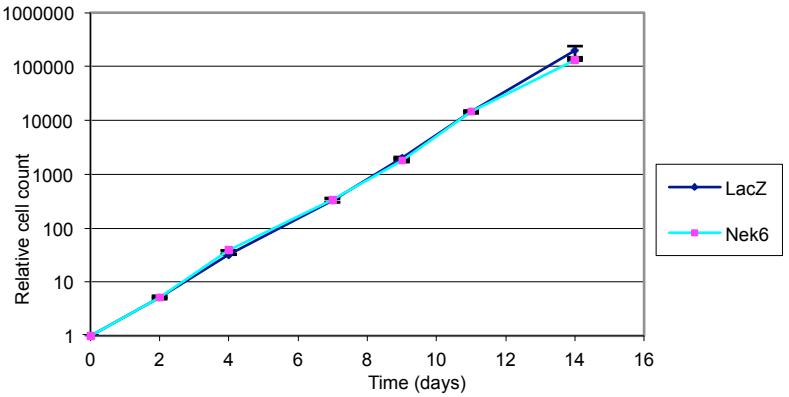

C

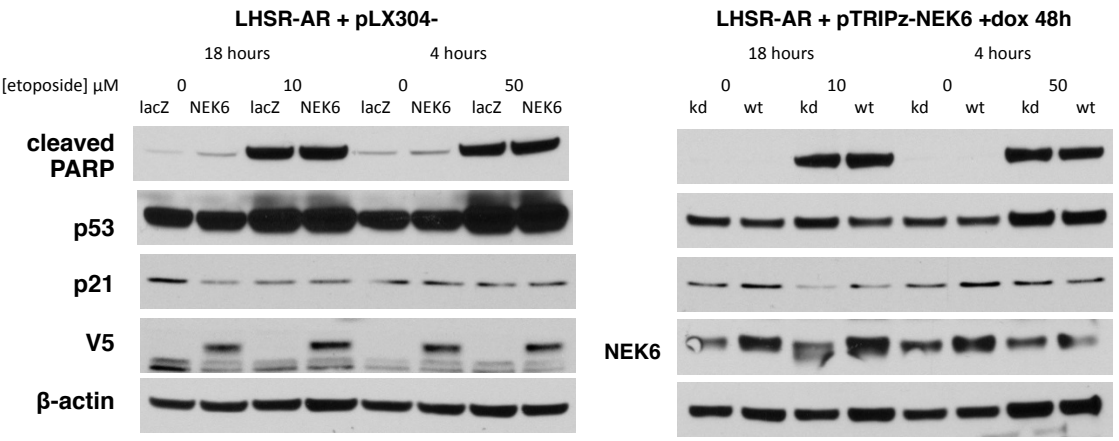

Supplemental Figure 4

A

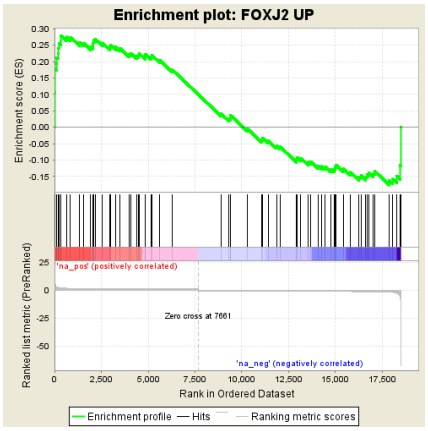

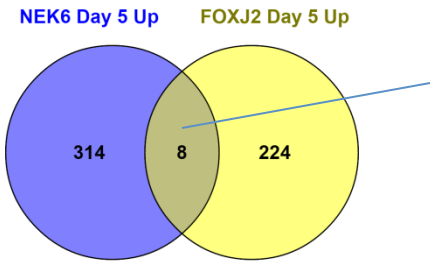

PLAC8
MAL
CRIP1
TPPP3
GSG1
PSCA
C14orf80
CCDC80

Enrichment Score (ES)	0.27894732
Normalized Enrichment Score (NES)	2.193419
Nominal p-value	0.002688172
FDR q-value	0.004374337
FWER p-Value	0.005

B

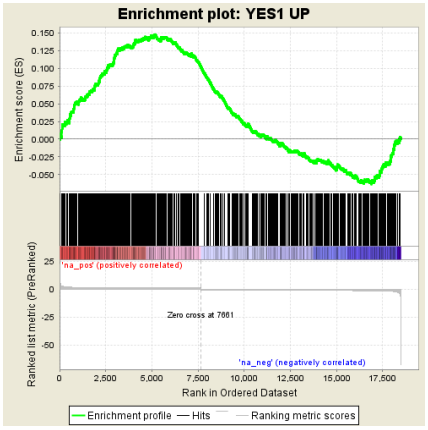

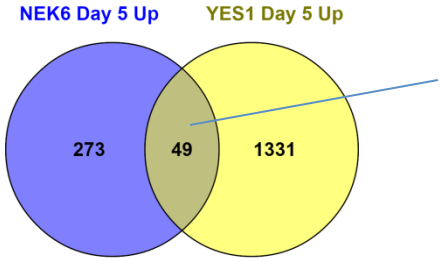

FKBP4
KRT19
KRT8
METRN
PGF
PLXNC1
SPDEF
CLU
RGCC
CFB
PHPT1
TNFSF9

Enrichment Score (ES)	0.14760399
Normalized Enrichment Score (NES)	2.1382623
Nominal p-value	0.0
FDR q-value	0.005037116
FWER p-Value	0.01

C

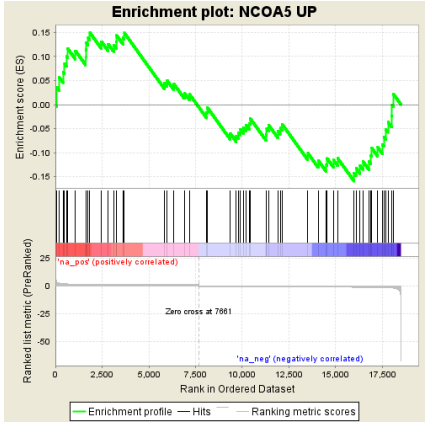

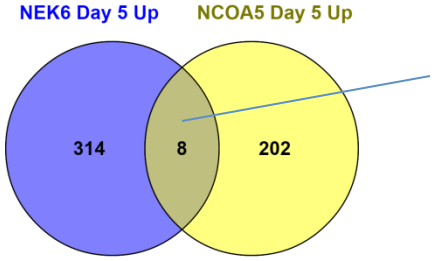

CTSW
C10orf55
GUSBP11
RP11-807G9.2
AC104698.1
CTD-2033A16.3
CBWD7
RP4-639F20.1

Enrichment Score (ES)	-0.15948276
Normalized Enrichment Score (NES)	-1.0333841
Nominal p-value	0.36886632
FDR q-value	0.4769835
FWER p-Value	0.913

Supplemental Figure 5

A

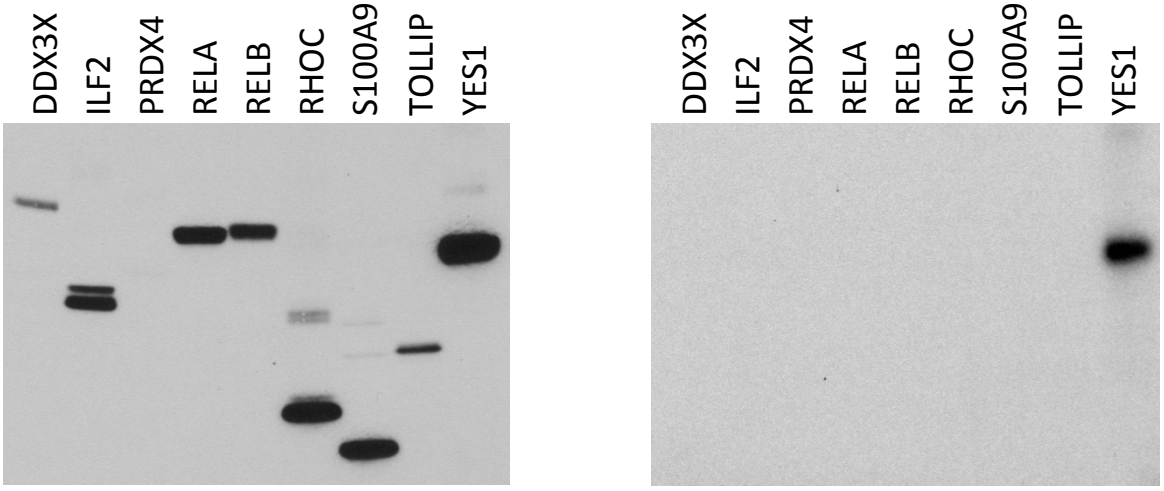

V5 **^{32}P-ATP**

B

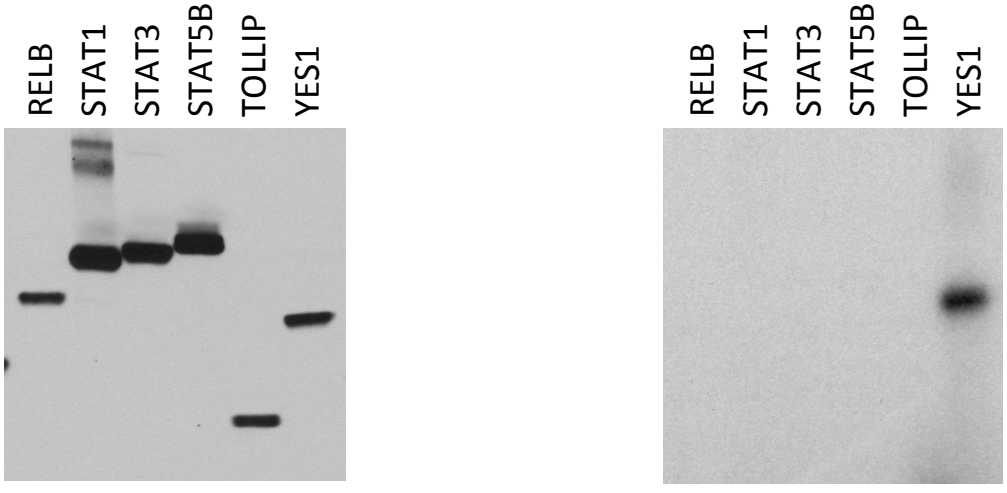

V5 **^{32}P-ATP**

Supplemental Figure 6